重力波宇宙論の展望

黒柳 幸子

(IFT UAM-CSIC / 名古屋大学)

２０２０年９月２日

素粒子物理学の進展２０２０

GW is the only way to directly observe the early universe

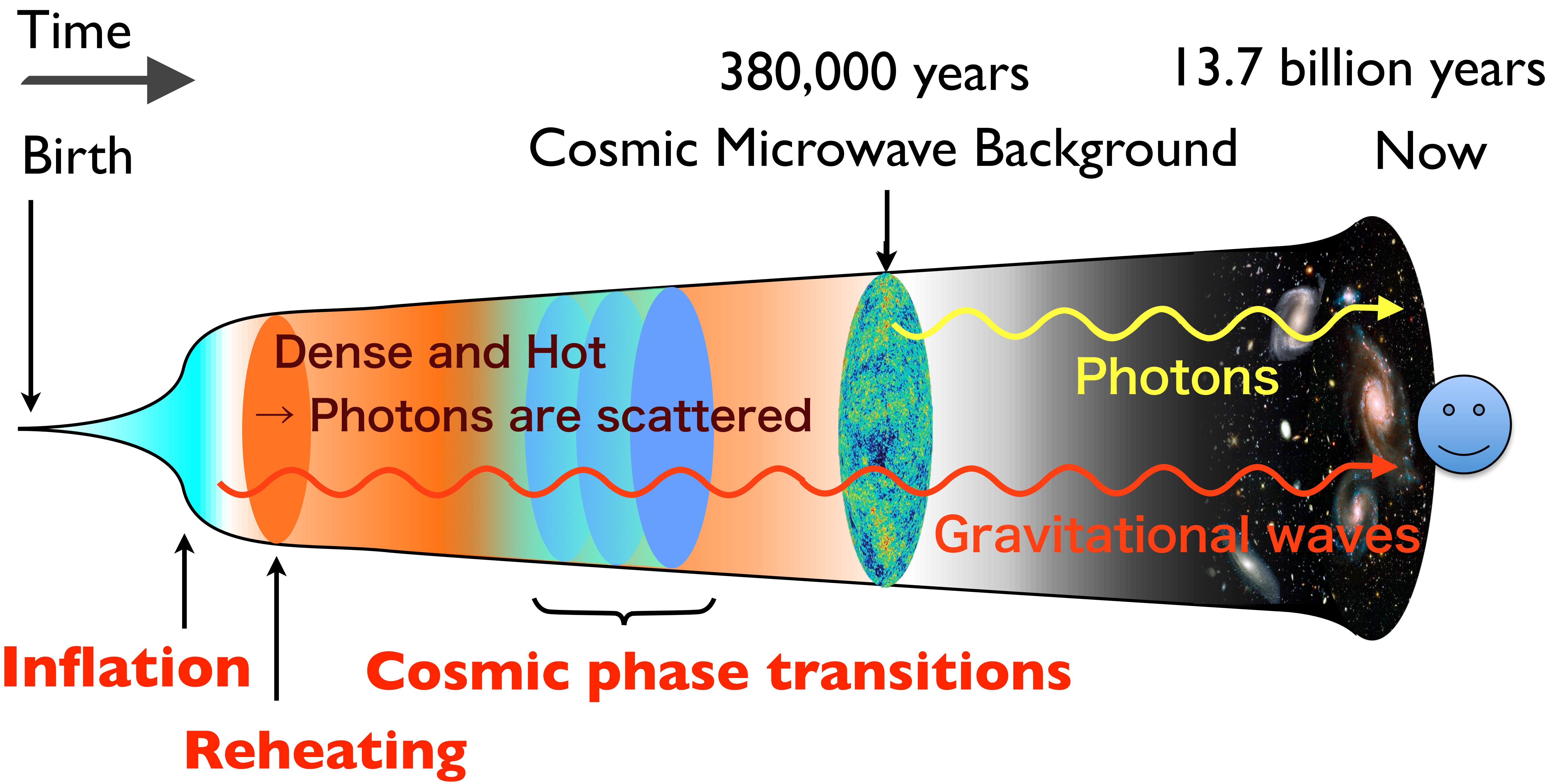

➡ **generate stochastic GWs**

Stochastic GW background

<u>Waveform</u>

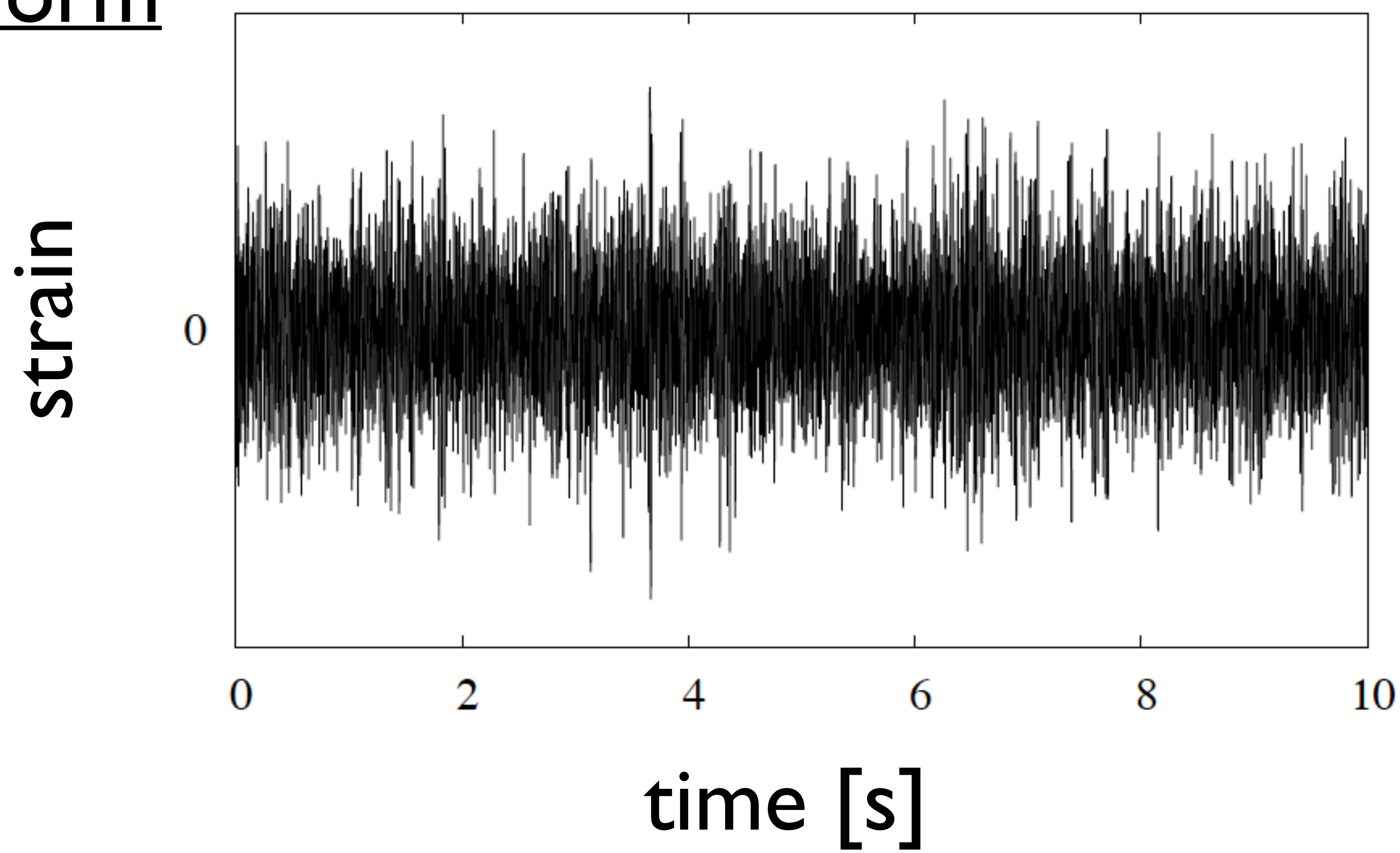

Continuous and random gravitational wave (GW) signal coming from all directions → very similar to noise

GW detectors in the world

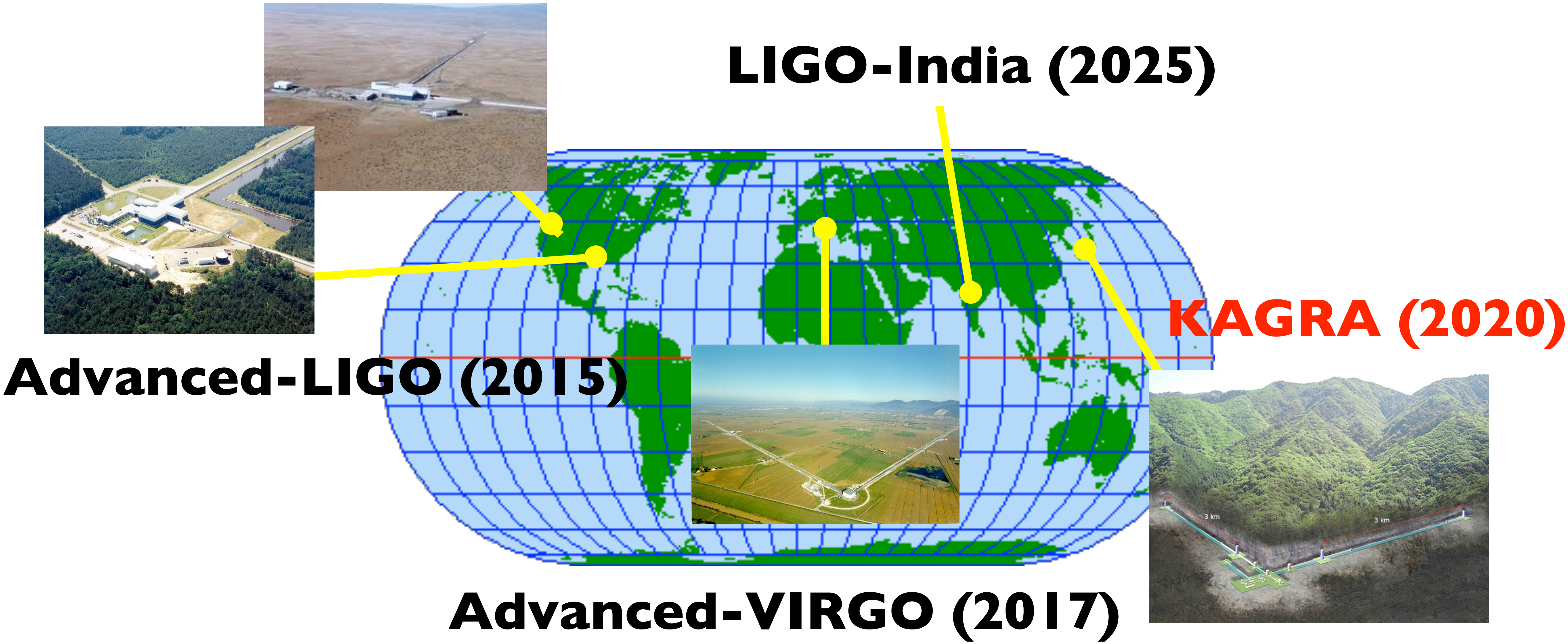

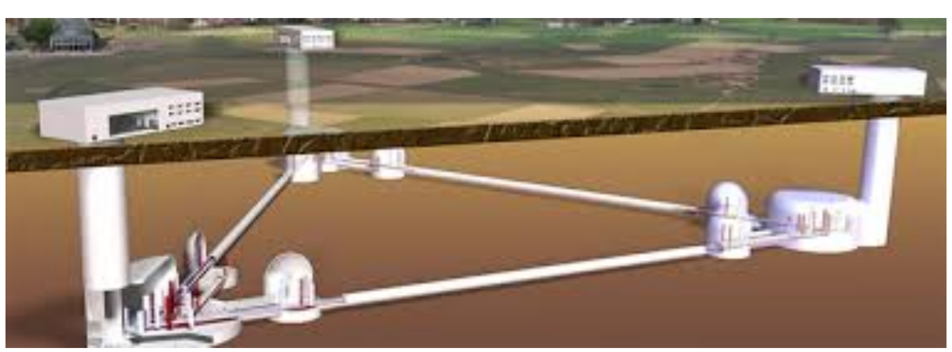

Future

LIGO A+, Voyager (2020')

Cosmic explorer
Einstein Telescope (2030')

Other GW experiments

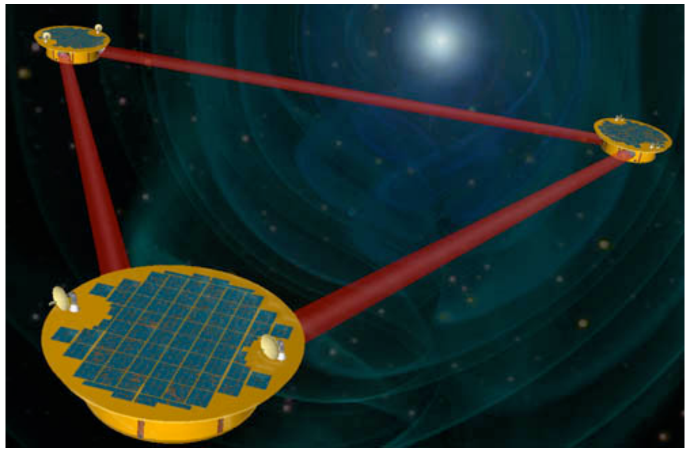

Space missions

LISA (2034)

DECIGO, TianQin, Taiji

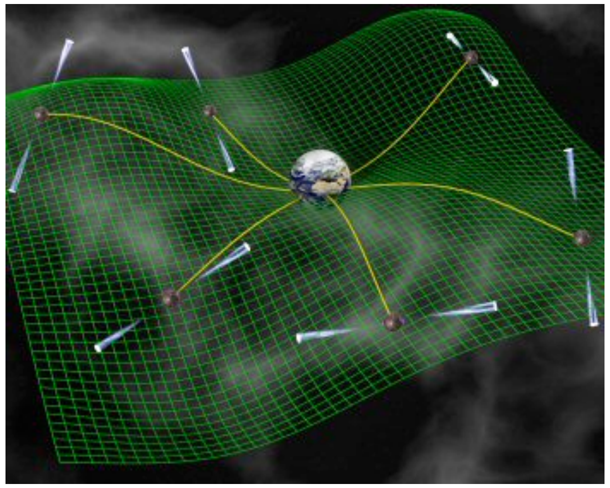

Pulsar timing array

ongoing: NANOGrav, EPTA, PPTA

SKA (2020-)

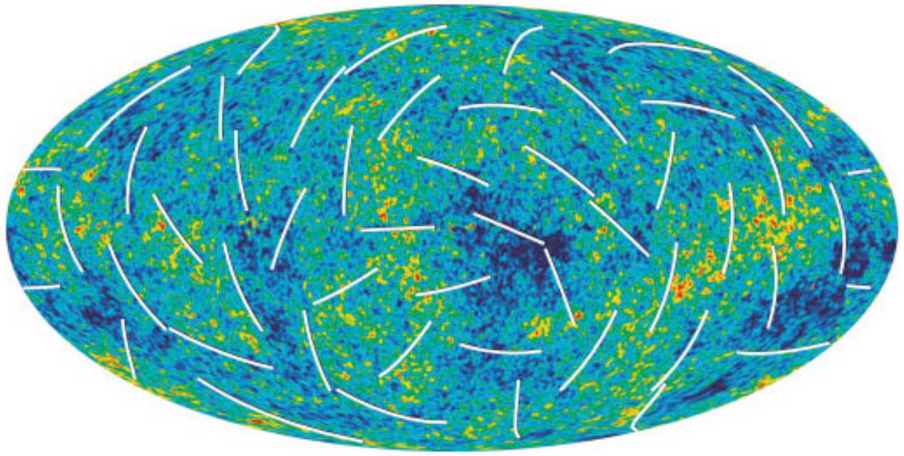

B-mode polarization in CMB

Ground-based experiments

LiteBIRD (2024-5?)

Generation mechanisms

Overlapped astrophysical GWs

interval of events $\Delta T < f^{-1}$

- Black hole binaries
- Neutron star binaries
- White dwarf binaries
- Supernovae

etc…

Cosmological GWs

generated in the early Universe

- Inflation
- Preheating
- Phase transitions
- Gauge fields
- Cosmic strings

etc…

GW generation

Evolution equation of GWs

$$\ddot{h}_{ij} + 3H\dot{h}_{ij} - \frac{1}{a^2}\nabla^2 h_{ij} = 16\pi G \Pi_{ij}$$

1. Non-negligible initial condition

- **Inflation**

→ quantum fluctuations in the spacetime

2. Sourced by matter component of the Universe

- **Preheating**

→ rapid particle productions

- **Phase transition**

→ bubble collisions

- **Cosmic strings**

→ heavy string objects generated at phase transition

GW generation

Evolution equation of GWs

$$\ddot{h}_{ij} + 3H\dot{h}_{ij} - \frac{1}{a^2}\nabla^2 h_{ij} = 16\pi G \Pi_{ij}$$

λ_{GW} < Hubble horizon size

$\rightarrow f/a < H$

Hubble horizon
= region of causality

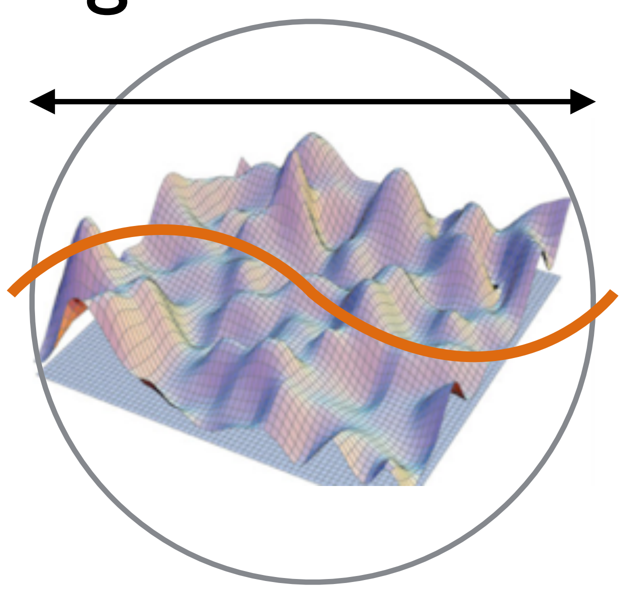

2. Sourced by matter component of the Universe

- **Preheating**
  → rapid particle productions
- **Phase transition**
  → bubble collisions
- **Cosmic strings**
  → heavy string objects generated in phase transition

GW spectrum and sensitivities

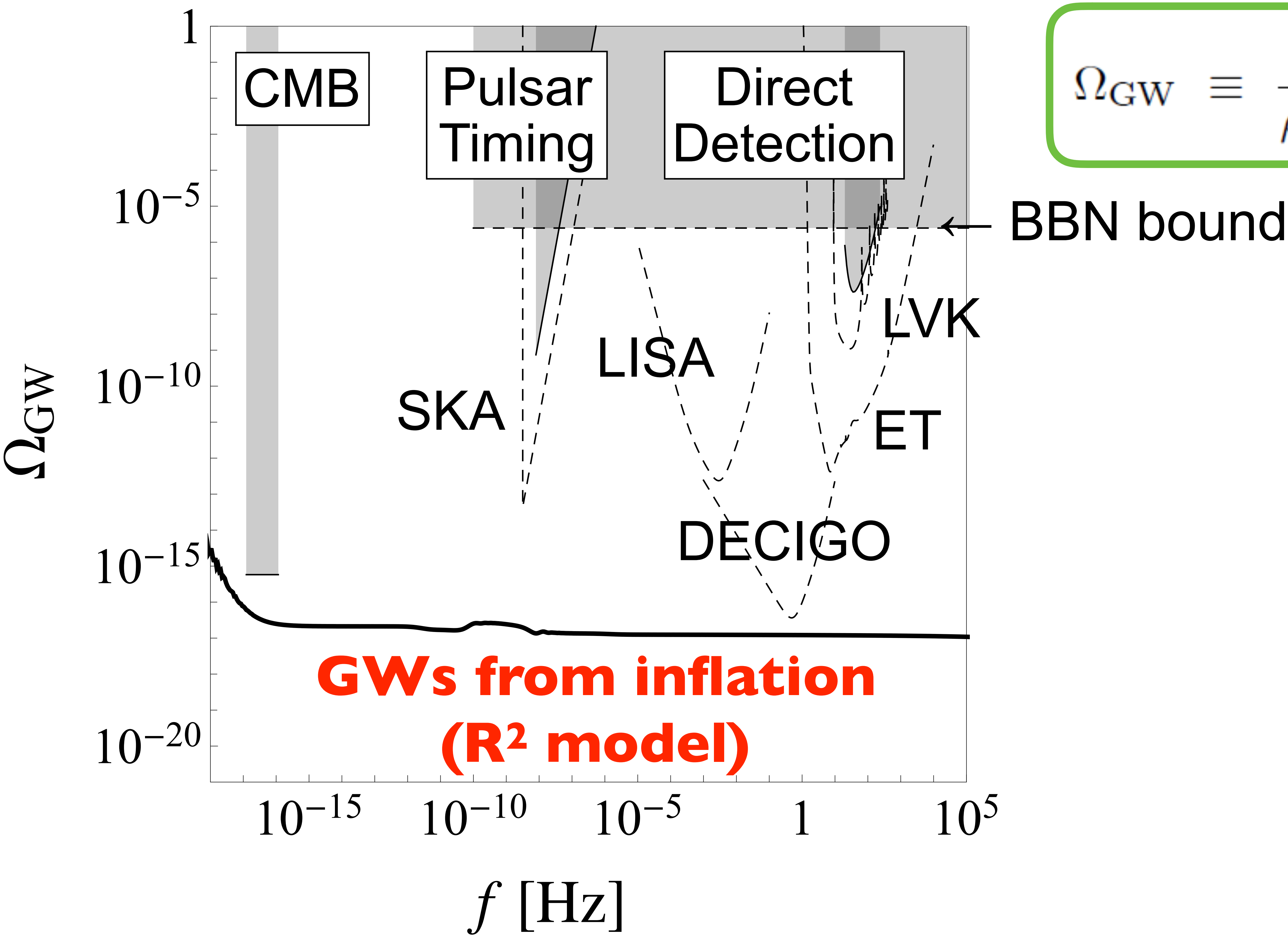

$$\Omega_{\rm GW} \equiv \frac{1}{\rho_c}\frac{d\rho_{\rm GW}}{d\ln k}$$

S. Kuroyanagi et al., PRD 79, 103501 (2009); PRD 90, 063513 (2014)

GW spectrum and sensitivities

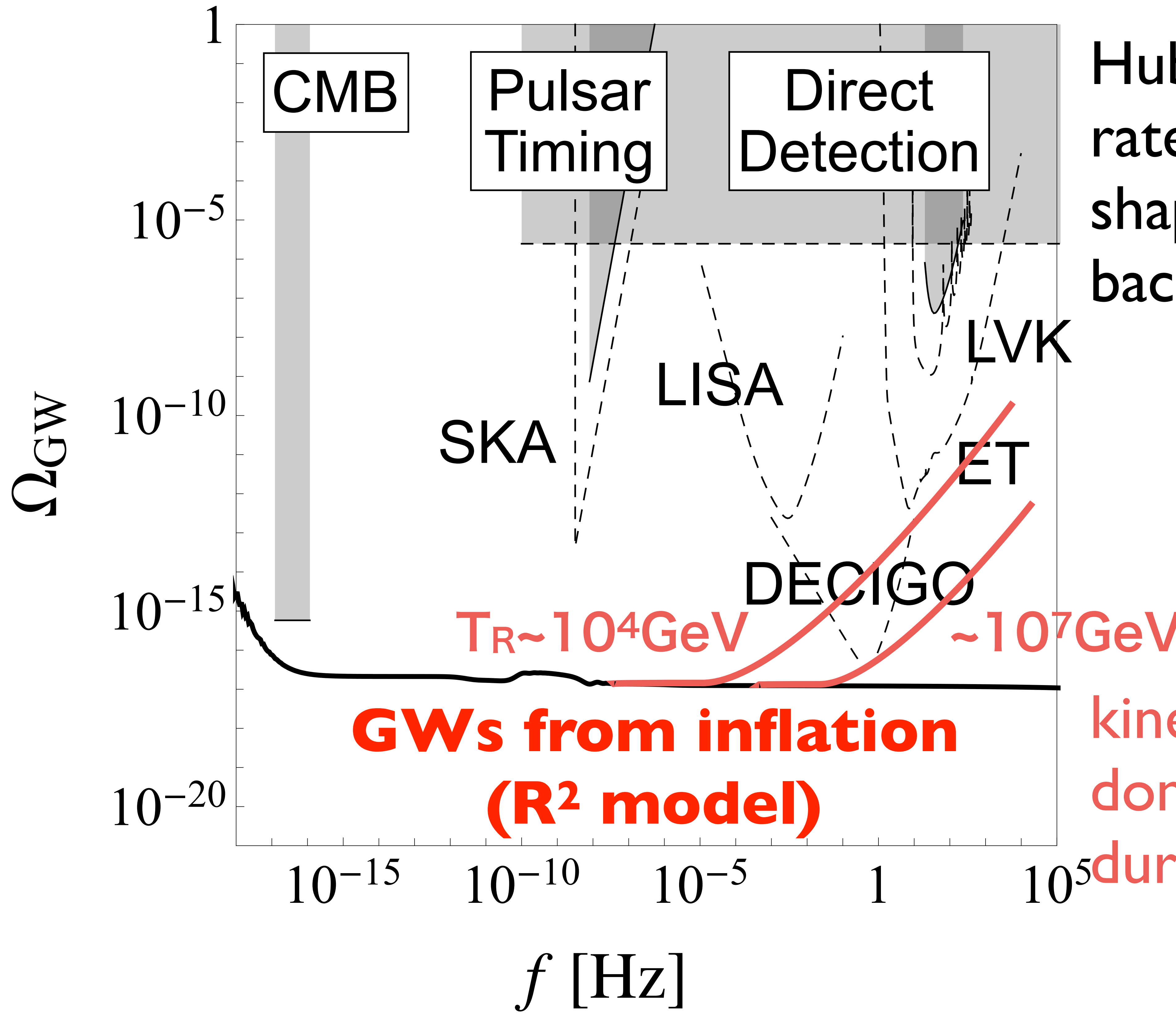

Hubble expansion rate affects the shape of the GW background

kinetic energy domination during reheating

S. Kuroyanagi et al., PRD 79, 103501 (2009); PRD 90, 063513 (2014)

Gauge field production during inflation

Inflation: accelerated expansion in the early Universe driven by a scalar field (inflaton)

coupling between inflaton and a gauge field

$$\Delta\mathcal{L}_{\rm int} = -\frac{1}{4f}\phi F_{\mu\nu}\tilde{F}^{\mu\nu}$$

→ the gauge field mode is amplified by $\sim e^{\pi\xi}$ $\quad \xi \equiv \frac{\dot{\phi}}{2fH}$

The anisotropic stress generates GWs

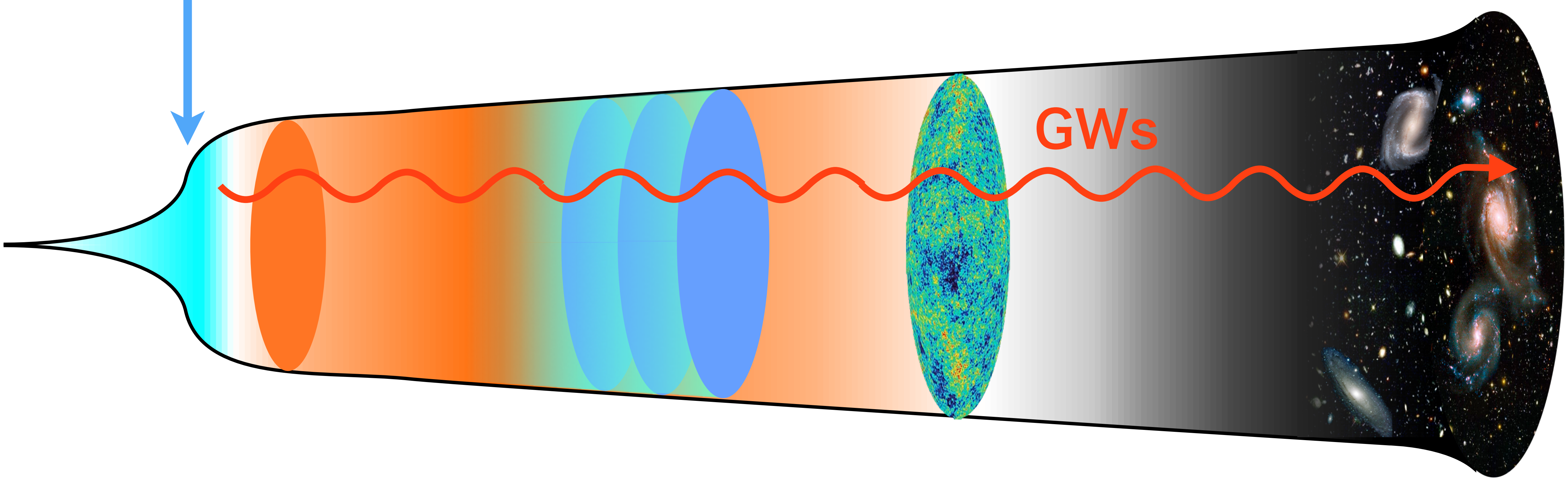

Gauge field production during inflation

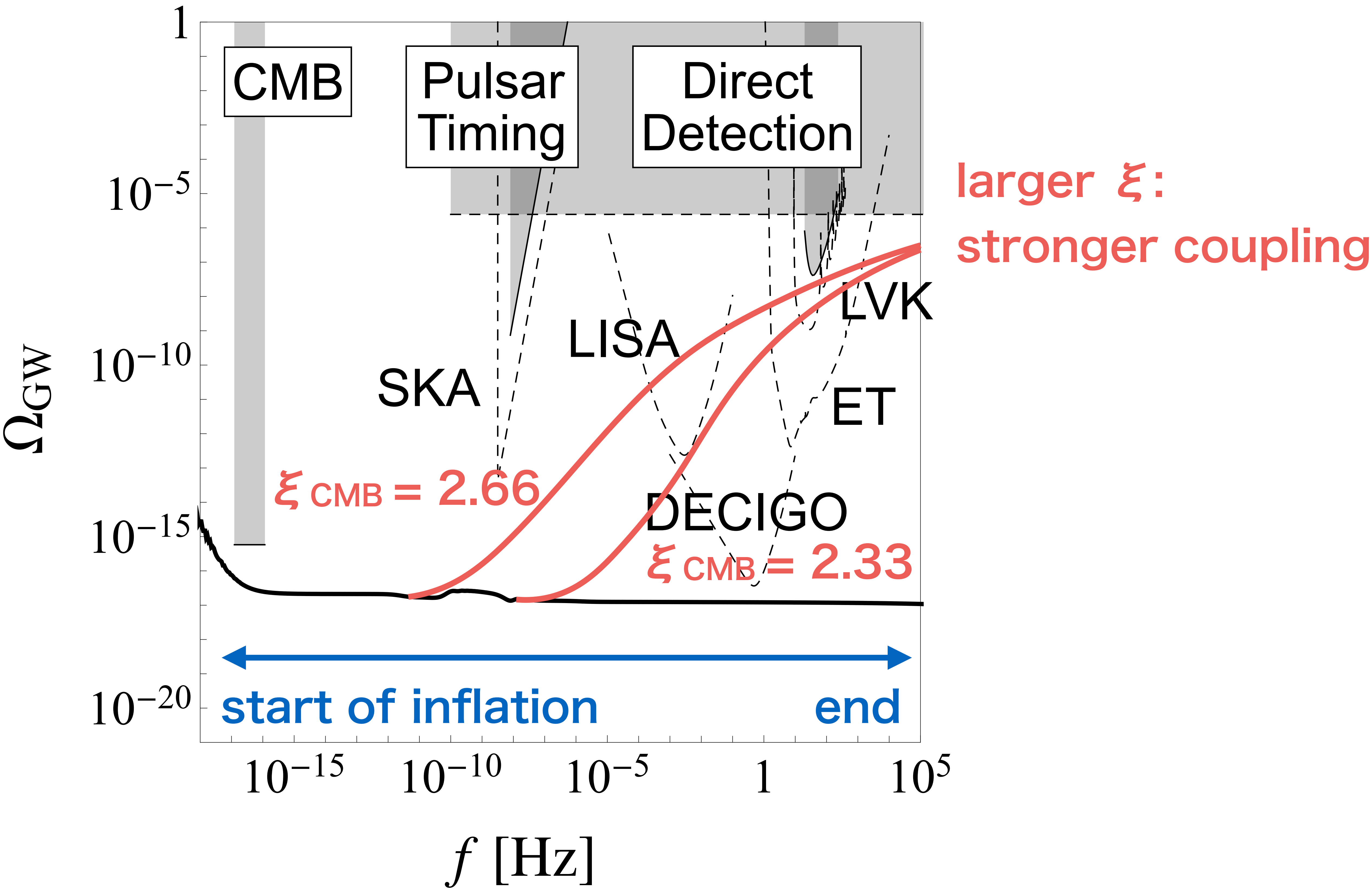

N. Barnaby et al., PRD 85 023525 (2012)

Primordial black holes

Prediction of CMB: $\mathcal{P}_{\mathcal{R}}(k) \sim 2\times 10^{-9}$ **at** $k \sim 0.05\mathrm{Mpc}^{-1}$

$\rightarrow f \sim 10^{-16}\mathrm{Hz}$

large primordial curvature perturbations at small scale can be produced by changing the dynamics of the inflaton

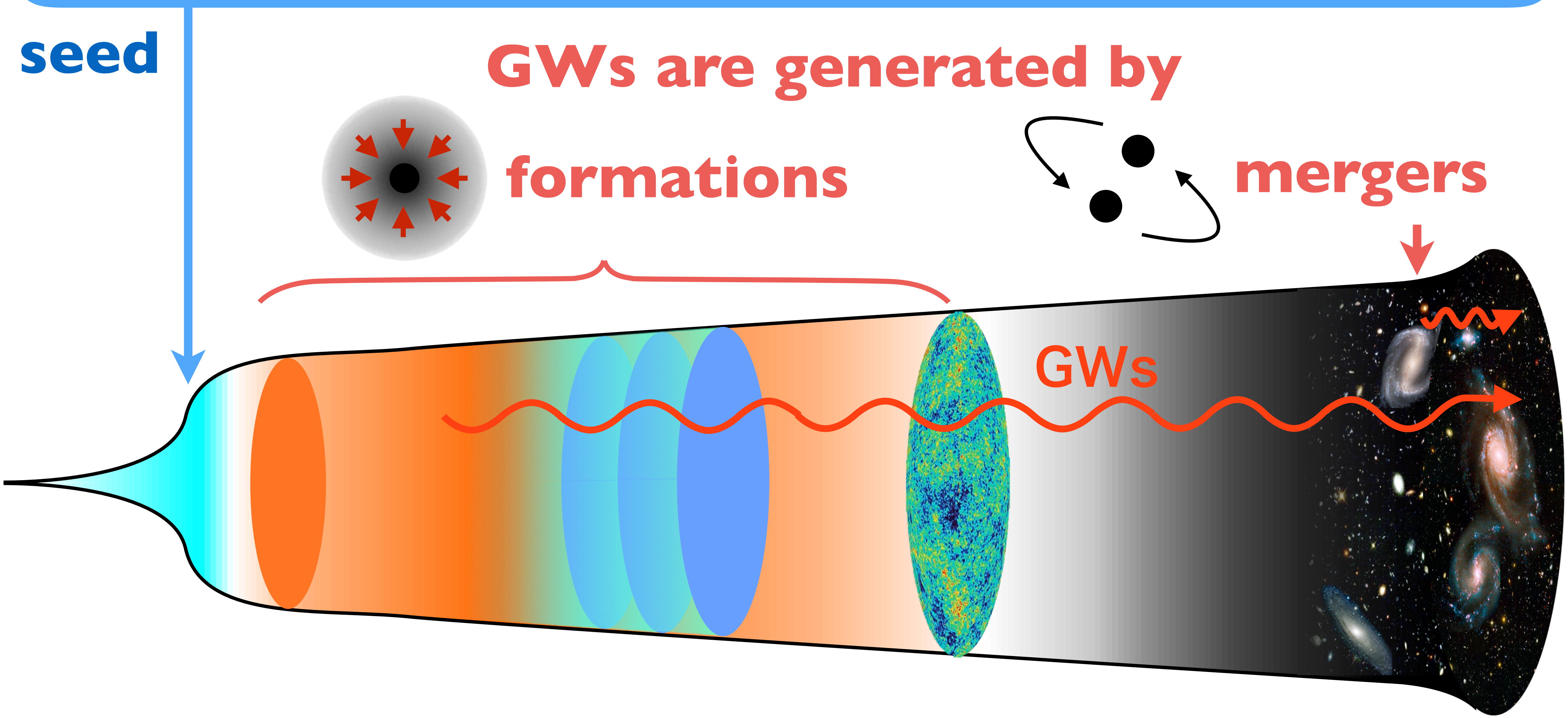

Primordial black holes: formation

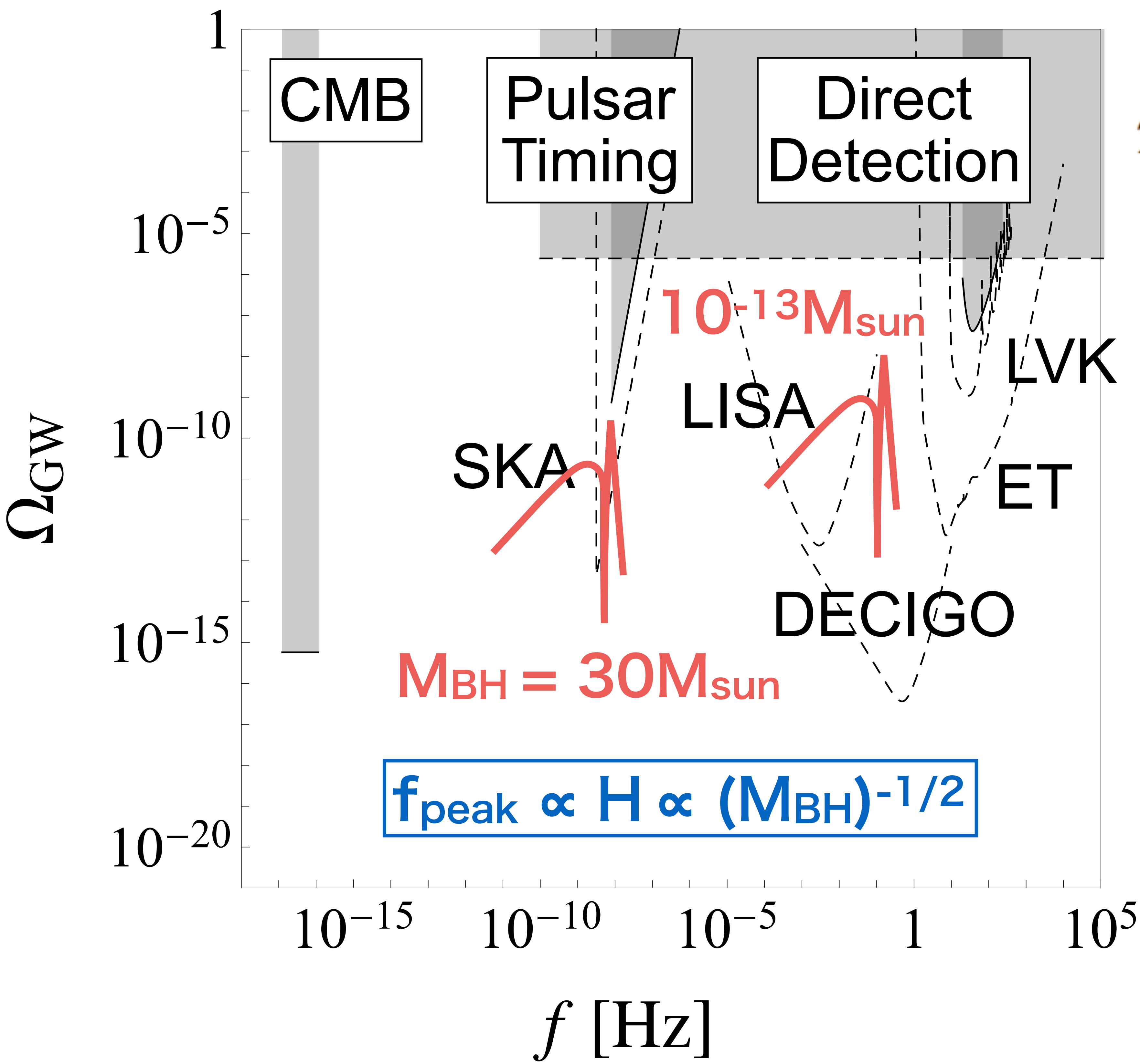

$$\mathcal{P}_{\Psi}(k) = \mathcal{A}^2 \delta_D(\ln(k/k_p))$$

δ function peak is assumed for curvature perturbations

R. Saito & J. Yokoyama, PRL 102, 161101 (2009)

Primordial black holes: merger

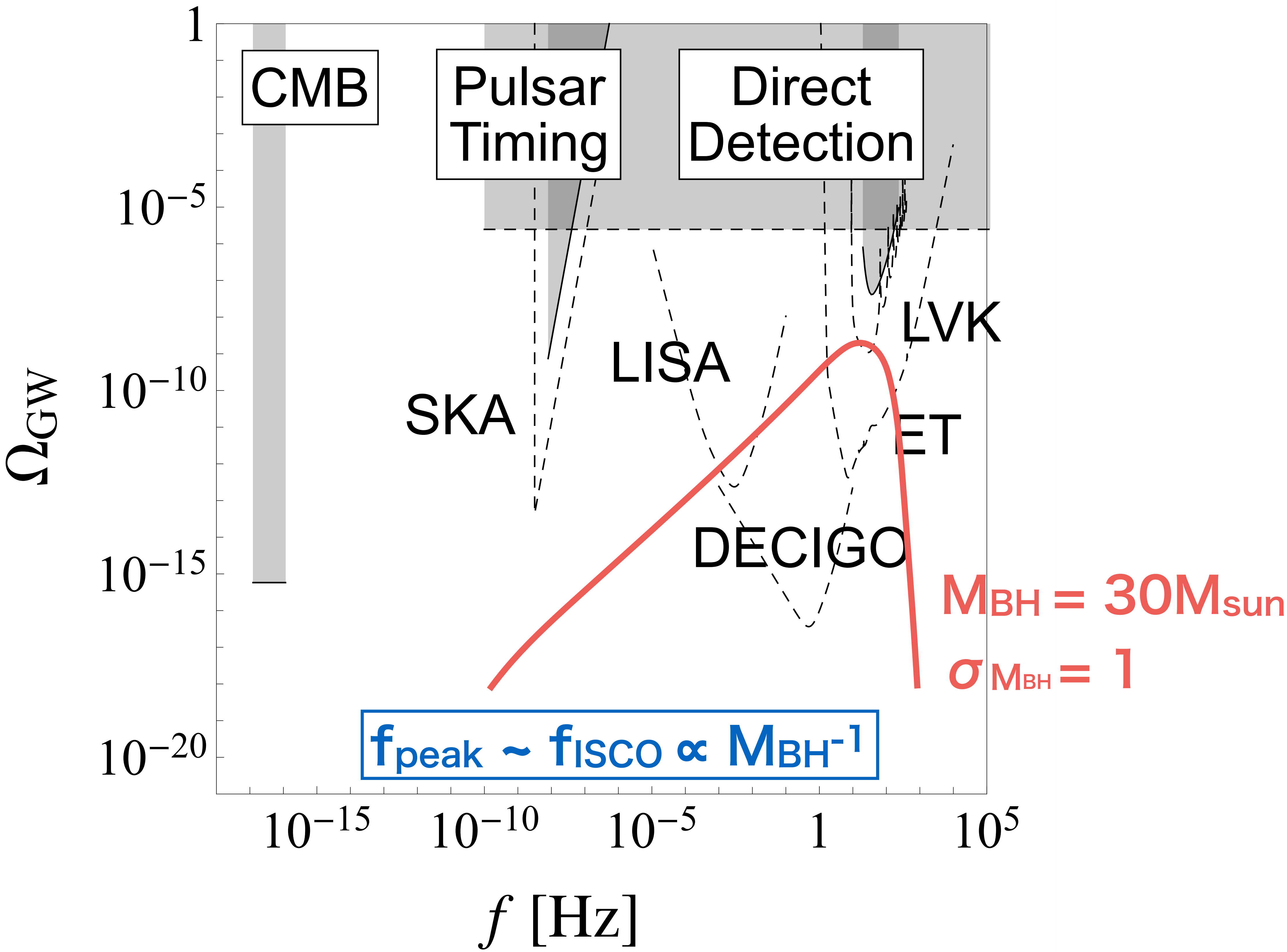

S. Clesse & J. García-Bellido, Phys. Dark Univ. 18 (2017) 105–114

Cosmic phase transitions

Bubbles appear in a first order phase transition

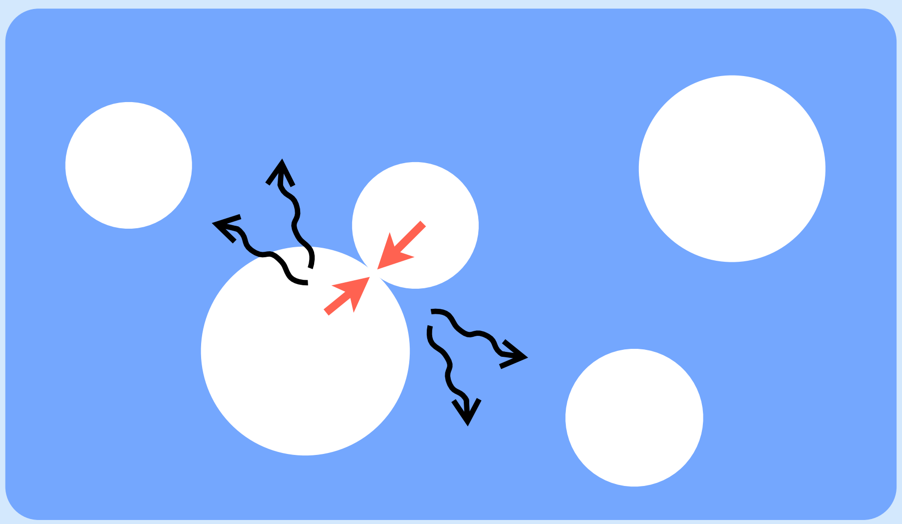

GWs are generated by

1. **collision of bubbles**
2. **sound waves ←dominant**
   (sourced by fluid kinetic energy)
3. **turbulence**
   (nonlinear process)

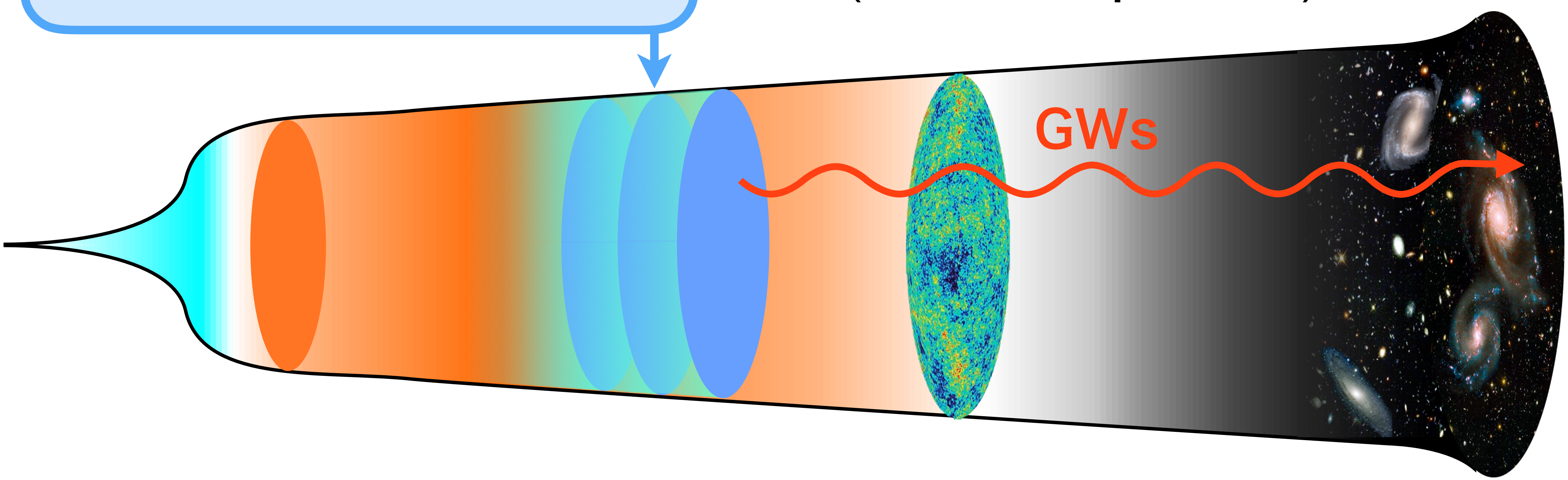

Cosmic phase transitions

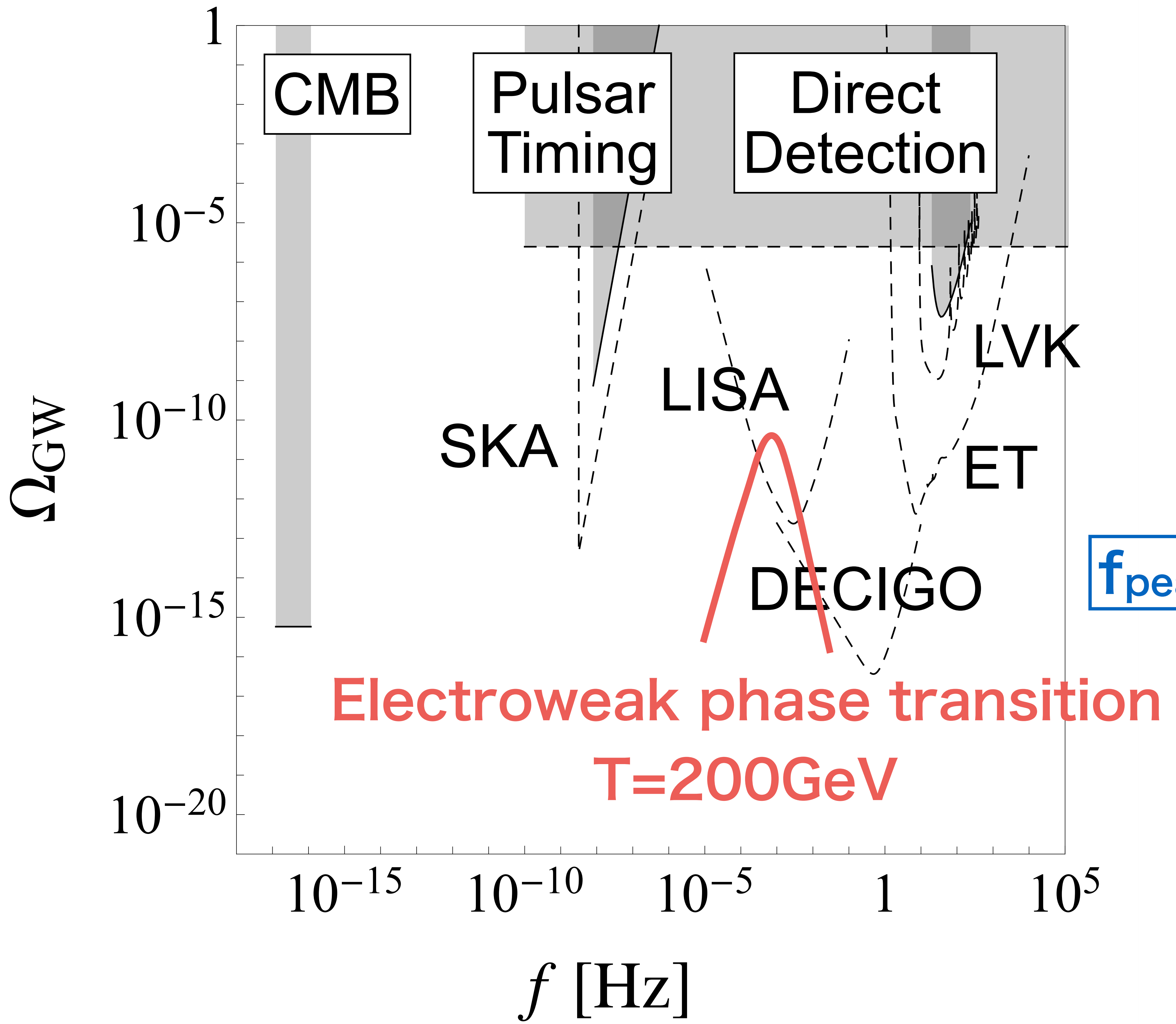

$f_{peak} \propto H \propto T$

C. Caprini et al. (LISA CosWG), JCAP 03 (2020) 024

Cosmic strings

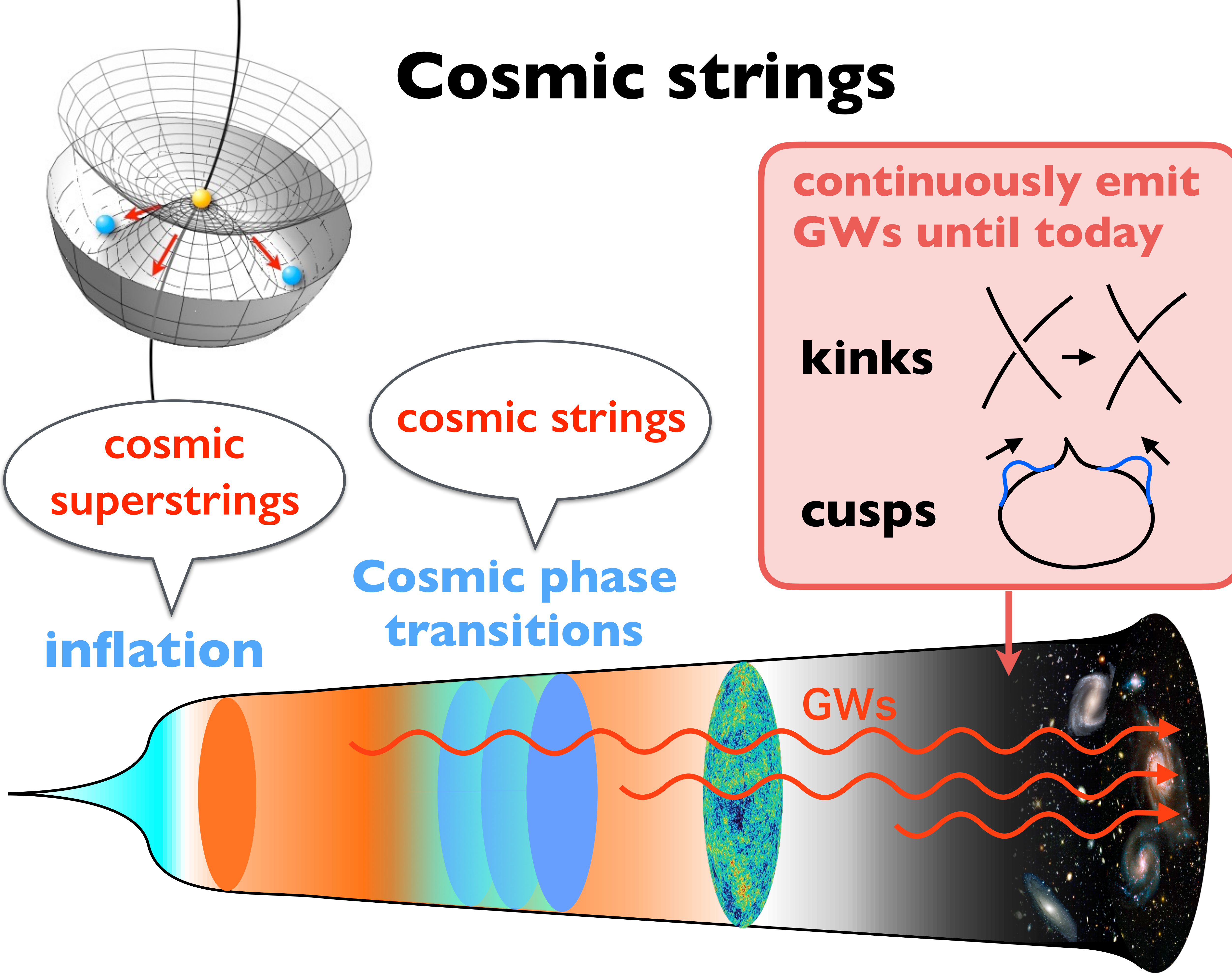

Cosmic strings (cusps on loops)

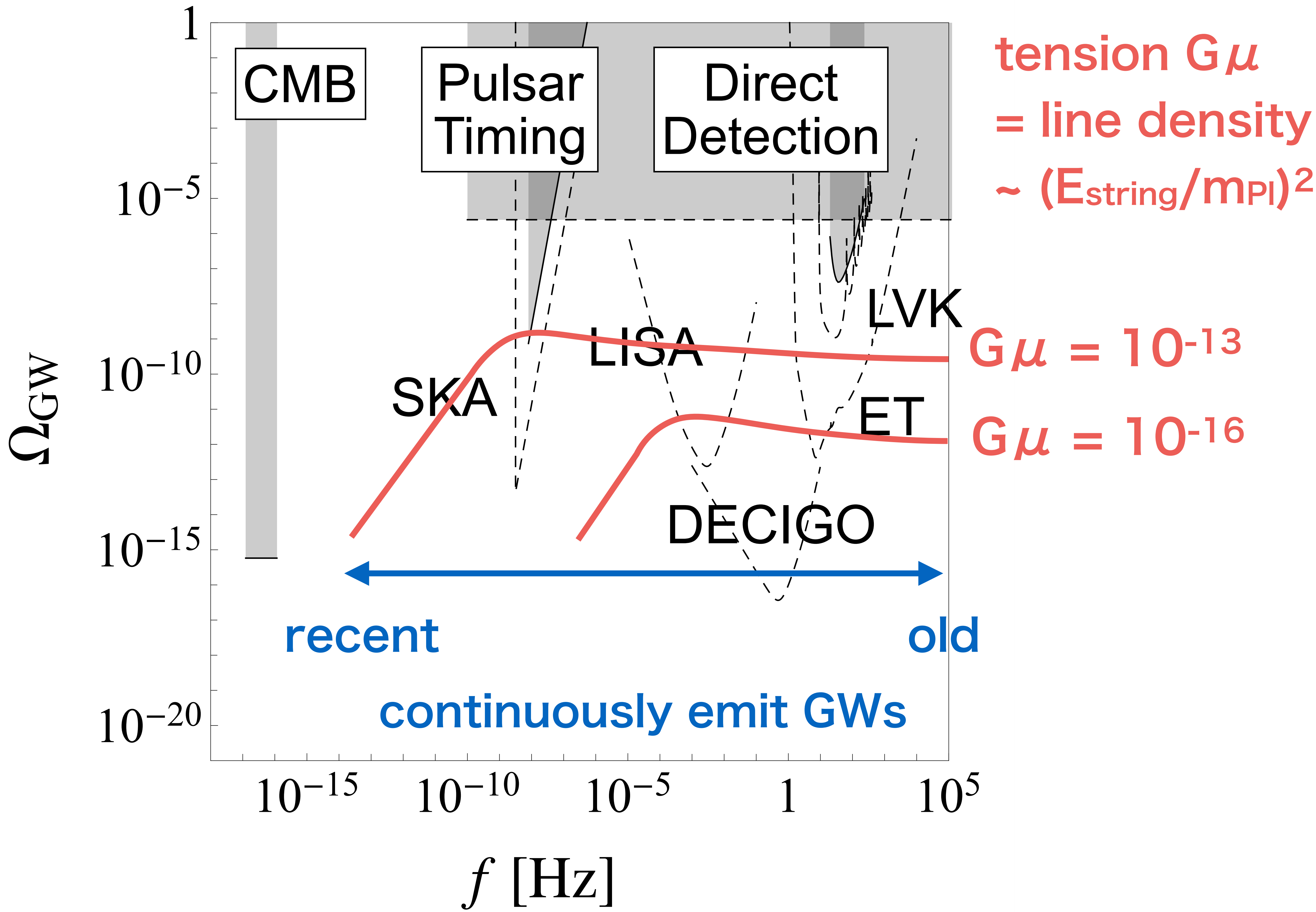

P. Auclair et al. (LISA CosWG), JCAP 04 (2020) 034

How can we determine the origin of the GW background?

→ go beyond the spectral amplitude and use other types of information such as

1. Spectral shape
2. Polarization
3. Anisotropy
4. Popcorn noise

(5. Non-Gaussianity)

How to detect a stochastic background

Cross Correlation

detector1	↔	detector2
$s_1(t) = h(t) + n_1(t)$		$s_2(t) = h(t) + n_2(t)$

s: observed signal
h: gravitational waves
n: noise

$$\langle S \rangle = \int_{-T/2}^{T/2} dt \, \langle s_1(t) s_2(t) \rangle$$

$$= \int_{-T/2}^{T/2} dt \, \langle h^2(t) + \underline{h(t)n_2(t) + n_1(t)h(t) + n_1(t)n_2(t)} \rangle$$

no correlations → 0

$$= \int_{-T/2}^{T/2} dt \, \underline{\langle h^2(t) \rangle}$$

GW signal

(for detectors at the same location)

Optimal filtering

B. Allen & J. Romano, PRD 59, 102001 (1999)

$$S := \int_{-T/2}^{T/2} dt \int_{-T/2}^{T/2} dt' \, s_1(t) s_2(t') \underline{Q(t,t')}$$

filter function

With the approximation $h \ll n$, the signal-to-noise ratio is

$$\mathrm{SNR}^2 = \frac{\mu^2}{\sigma^2} \approx \left(\frac{3H_0^2}{10\pi^2}\right)^2 T \frac{\left(\underline{\tilde{Q}}, \frac{\gamma(|f|)\Omega_{\mathrm{gw}}(|f|)}{|f|^3 P_1(|f|) P_2(|f|)}\right)^2}{\underline{(\tilde{Q},\tilde{Q})}}$$

$$(A,B) := \int_{-\infty}^{\infty} df \, A^*(f) B(f) P_1(|f|) P_2(|f|)$$

filter function in Fourier space

SNR is maximized when

$$\tilde{Q}(f) = \lambda \frac{\gamma(|f|)\Omega_{\mathrm{gw}}(|f|)}{|f|^3 P_1(|f|) P_2(|f|)}$$

Optimal filtering

B. Allen & J. Romano, PRD 59, 102001 (1999)

SNR is maximized when

$$\tilde{Q}(f) = \lambda \frac{\gamma(|f|)\,\Omega_{\rm gw}(|f|)}{|f|^3 P_1(|f|)\,P_2(|f|)}$$

Optimal filtering

B. Allen & J. Romano, PRD 59, 102001 (1999)

SNR is maximized when

$$\tilde{Q}(f) = \lambda \frac{\gamma(|f|)\Omega_{\mathrm{gw}}(|f|)}{|f|^3 P_1(|f|) P_2(|f|)}$$

$n(t) \to P_i(|f|)$: noise spectrum

observable:

$$s(t) = h(t) + n(t) \sim n(t)$$

$h \ll n$

$\to$ **obtained from data**

Optimal filtering

B. Allen & J. Romano, PRD 59, 102001 (1999)

SNR is maximized when

$$\tilde{Q}(f) = \lambda \frac{\gamma(|f|)\Omega_{\rm gw}(|f|)}{|f|^3 P_1(|f|) P_2(|f|)}$$

$h(t) \to \Omega_{\rm gw}(|f|)$: GW spectrum

$\to$ unknown

$\to$ We prepare
a template bank
of spectral shape

$n(t) \to P_i(|f|)$: noise spectrum

observable:

$$s(t) = h(t) + n(t) \sim n(t)$$

↑ $h \ll n$

$\to$ obtained from data

Optimal filtering

B. Allen & J. Romano, PRD 59, 102001 (1999)

SNR is maximized when

$$\tilde{Q}(f) = \lambda \frac{\gamma(|f|)\,\Omega_{gw}(|f|)}{|f|^3 P_1(|f|) P_2(|f|)}$$

overlap reduction function

determined by detector response

$h(t) \rightarrow \Omega_{gw}(|f|)$: GW spectrum

$\rightarrow$ **unknown**

$\rightarrow$ **We prepare**
a template bank
of spectral shape

$n(t) \rightarrow P_i(|f|)$: noise spectrum

observable:

$$s(t) = h(t) + n(t) \sim n(t)$$

$h \ll n$

$\rightarrow$ **obtained from data**

Detector response

Sensitivity of an interferometer depends on **source location** and **polarization**

observable: $s(t) = \underline{F(\hat{\mathbf{\Omega}})}h(t) + n(t)$

response function

$\hat{\mathbf{\Omega}}$: direction of GW propagation

+ mode

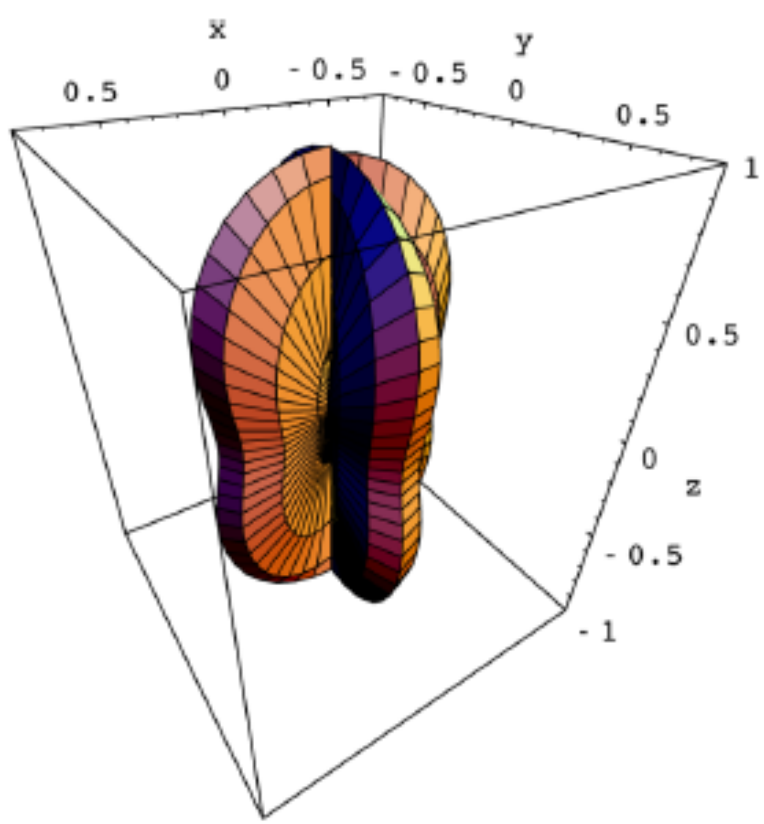

detector arms

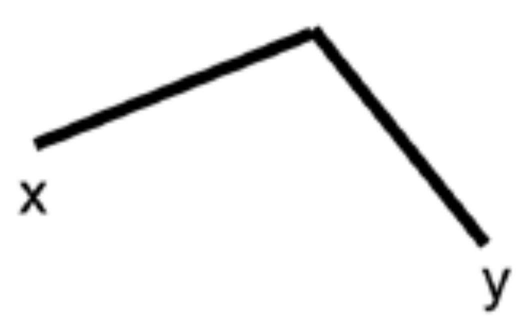

× mode

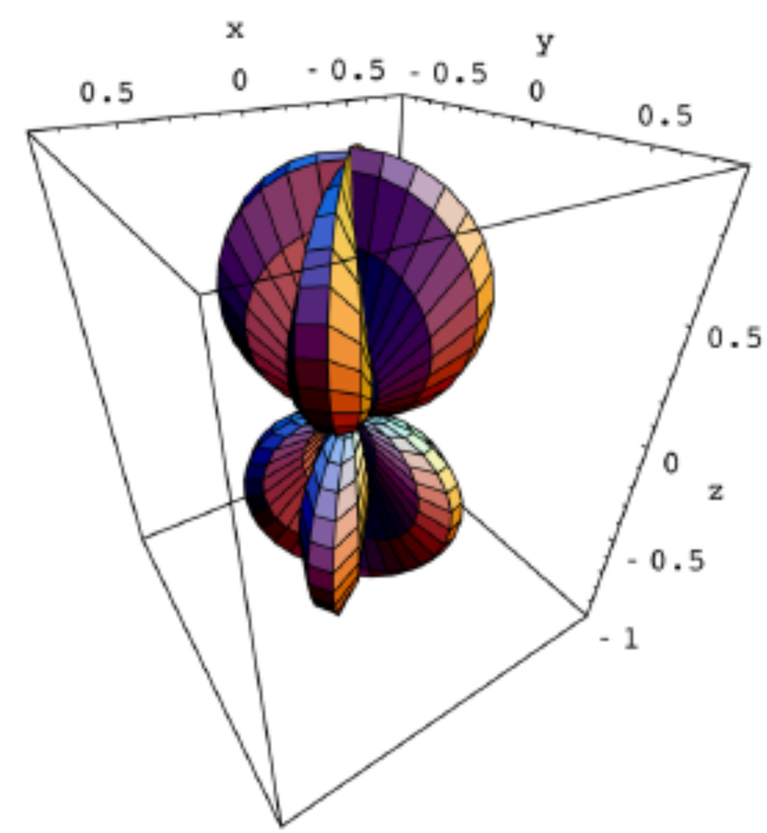

Figure from A. Nishizawa et al. PRD 79, 082002 (2009)

Overlap reduction function

For a stochastic GW background, we construct

$$\gamma_{IJ}^{T}(f) \equiv \frac{5}{2}\int_{S^2}\frac{d\hat{\Omega}}{4\pi}e^{2\pi i f\hat{\Omega}\cdot\Delta\vec{X}/c}(F_I^{+}F_J^{+}+F_I^{\times}F_J^{\times})$$

integration over the whole sky

separation of detectors

response function

I and J denote different detectors

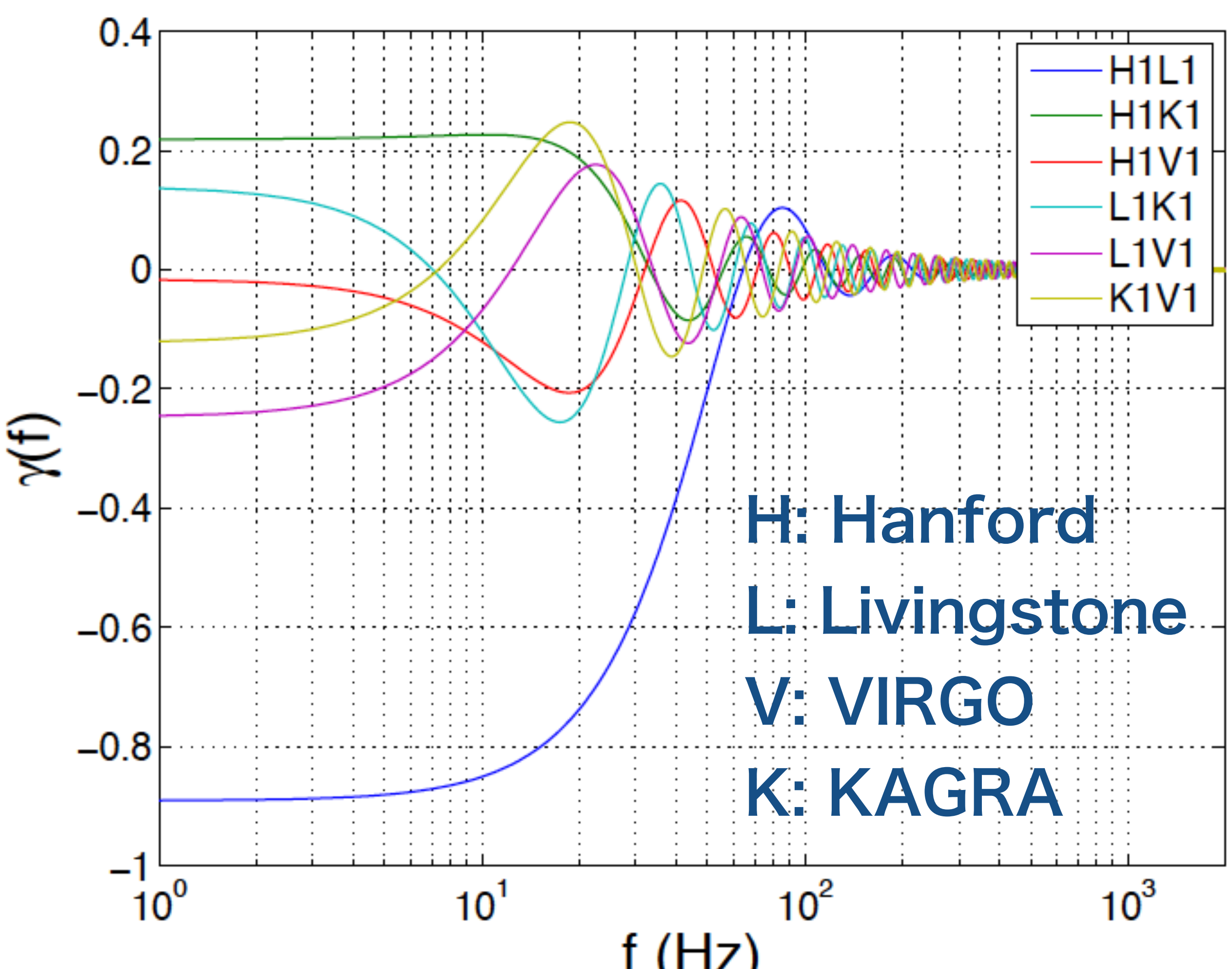

→ represents the amount of preserved correlation between two detectors

E. Thrane & J. D. Romano, PRD 88, 124032 (2013)

I. Spectral shape

GW background is searched by changing
spectral shape template

filter function

$$\tilde{Q}(f) = \lambda \frac{\gamma(|f|)\Omega_{gw}(|f|)}{|f|^3 P_1(|f|) P_2(|f|)}$$

usually parametrized by a single power law

$$\Omega_{GW}(f) = \Omega_\alpha \left(\frac{f}{f_{ref}}\right)^\alpha$$

$$f_{ref} = 25\mathrm{Hz}$$

LIGO & Virgo Collaboration, PRL 118, 121101 (2017)

→ but many models of GW background predict a peaked shape

Multi-binning reconstruction

- Spectral tilt is fitted in each bin
- Binning is optimized by calculating the AIC

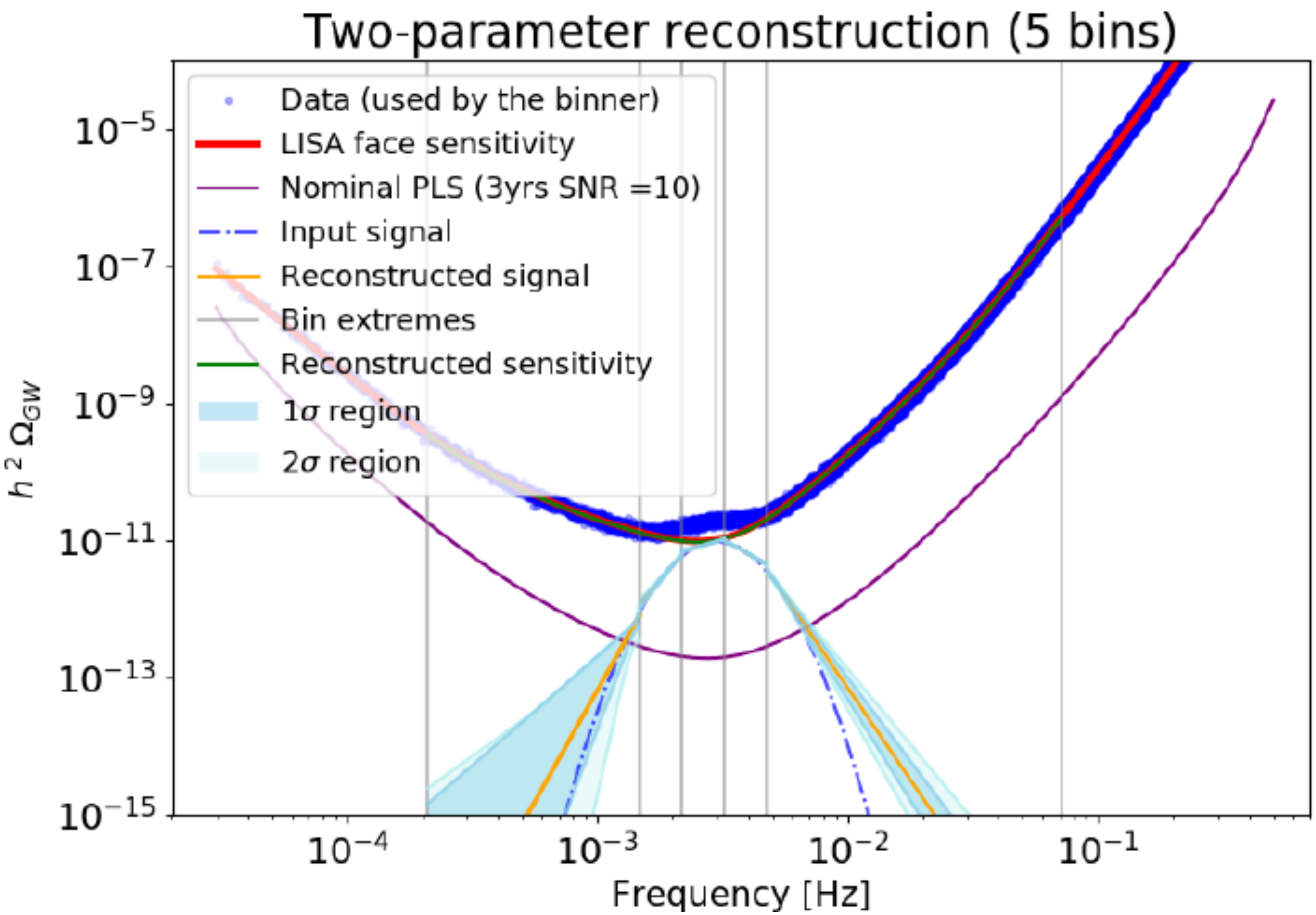

C. Caprini et al. (LISA CosWG), JCAP 11 017 (2019)

Multi-binning reconstruction

- Spectral tilt is fitted in each bin
- Binning is optimized by calculating the AIC

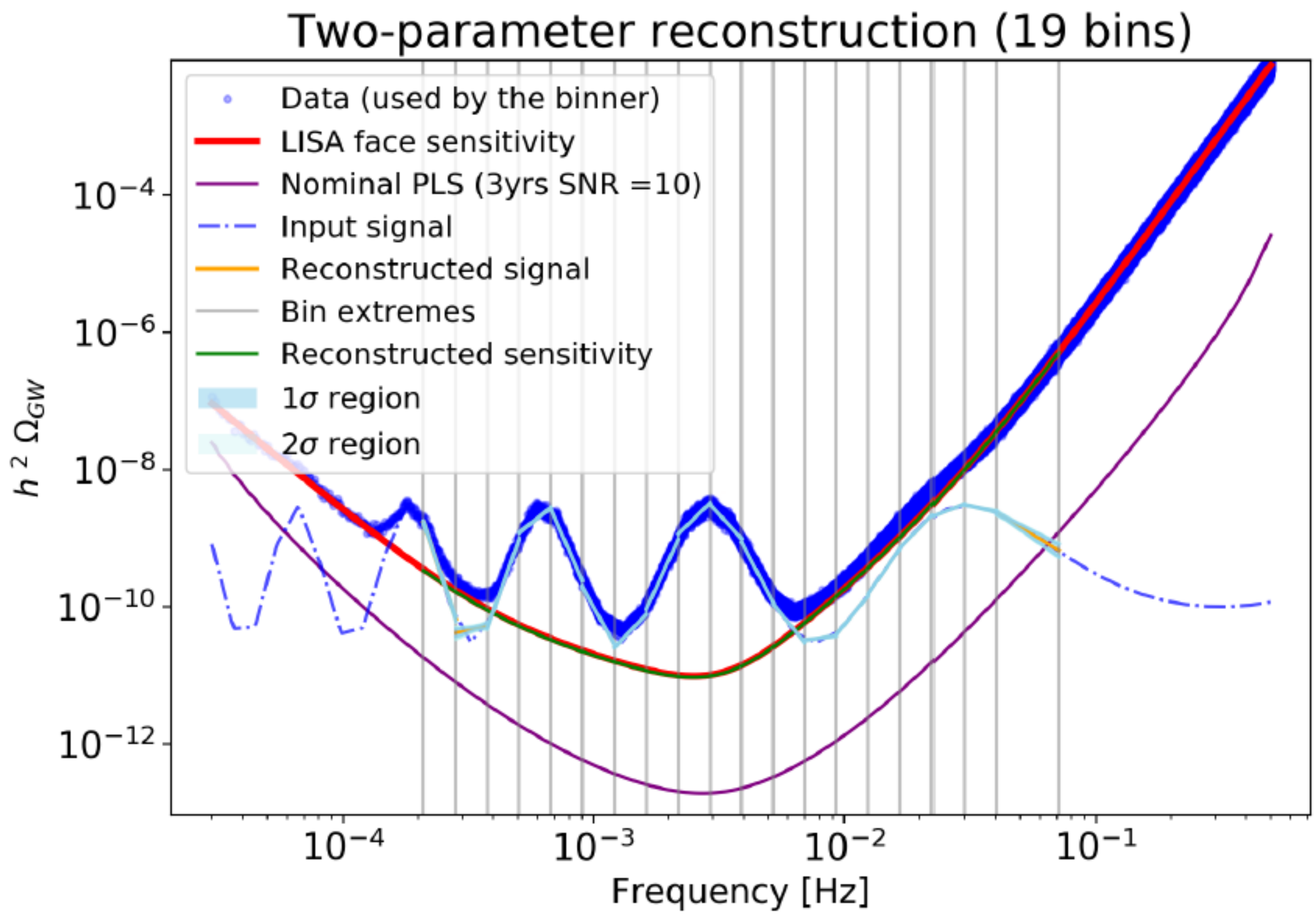

C. Caprini et al. (LISA CosWG), JCAP 11 017 (2019)

2. Polarization

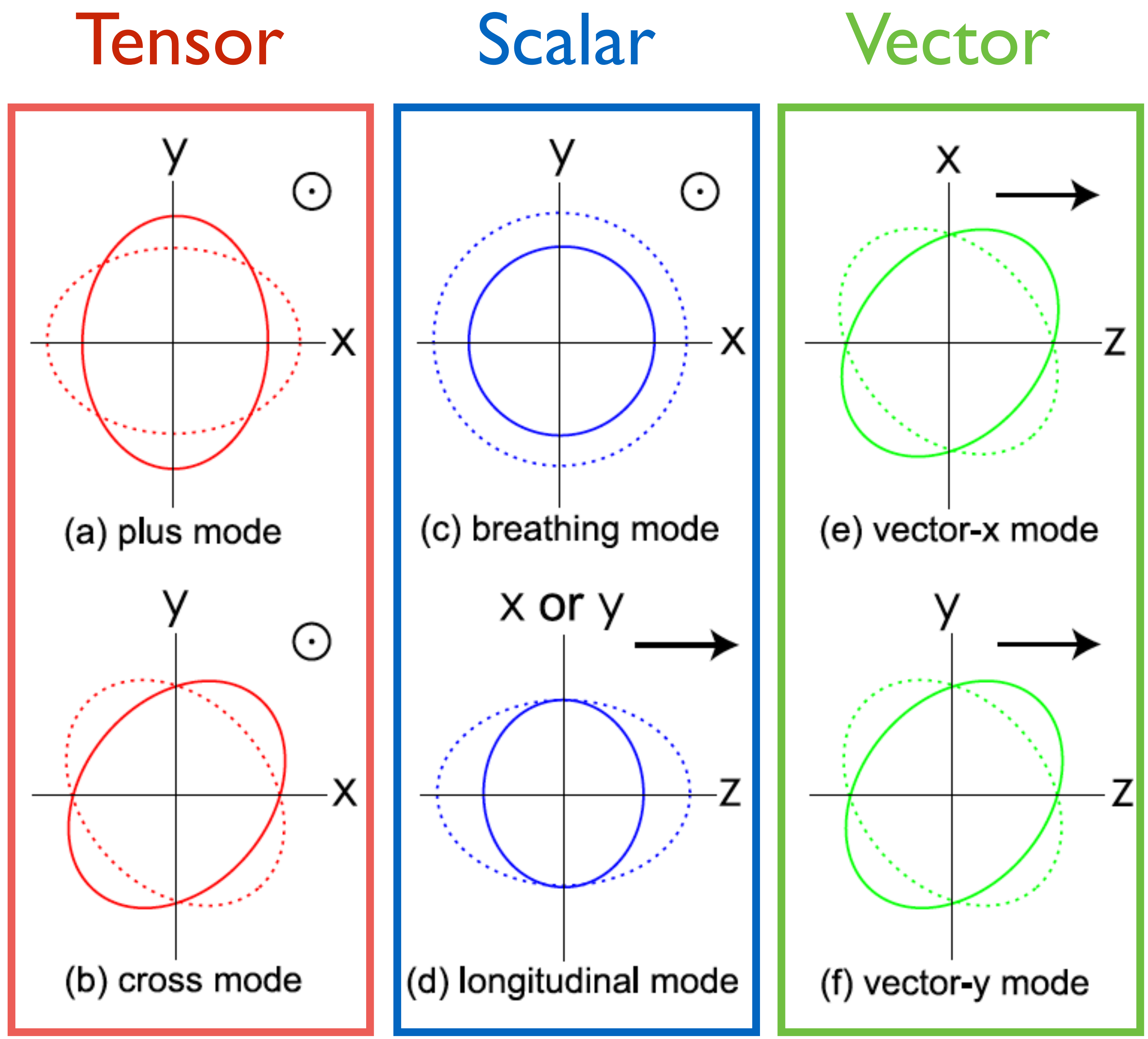

Linear + Circular modes

→ probe of non-GR

A. Nishizawa et al. PRD 79, 082002 (2009)

How can we detect polarization?

Detector response changes

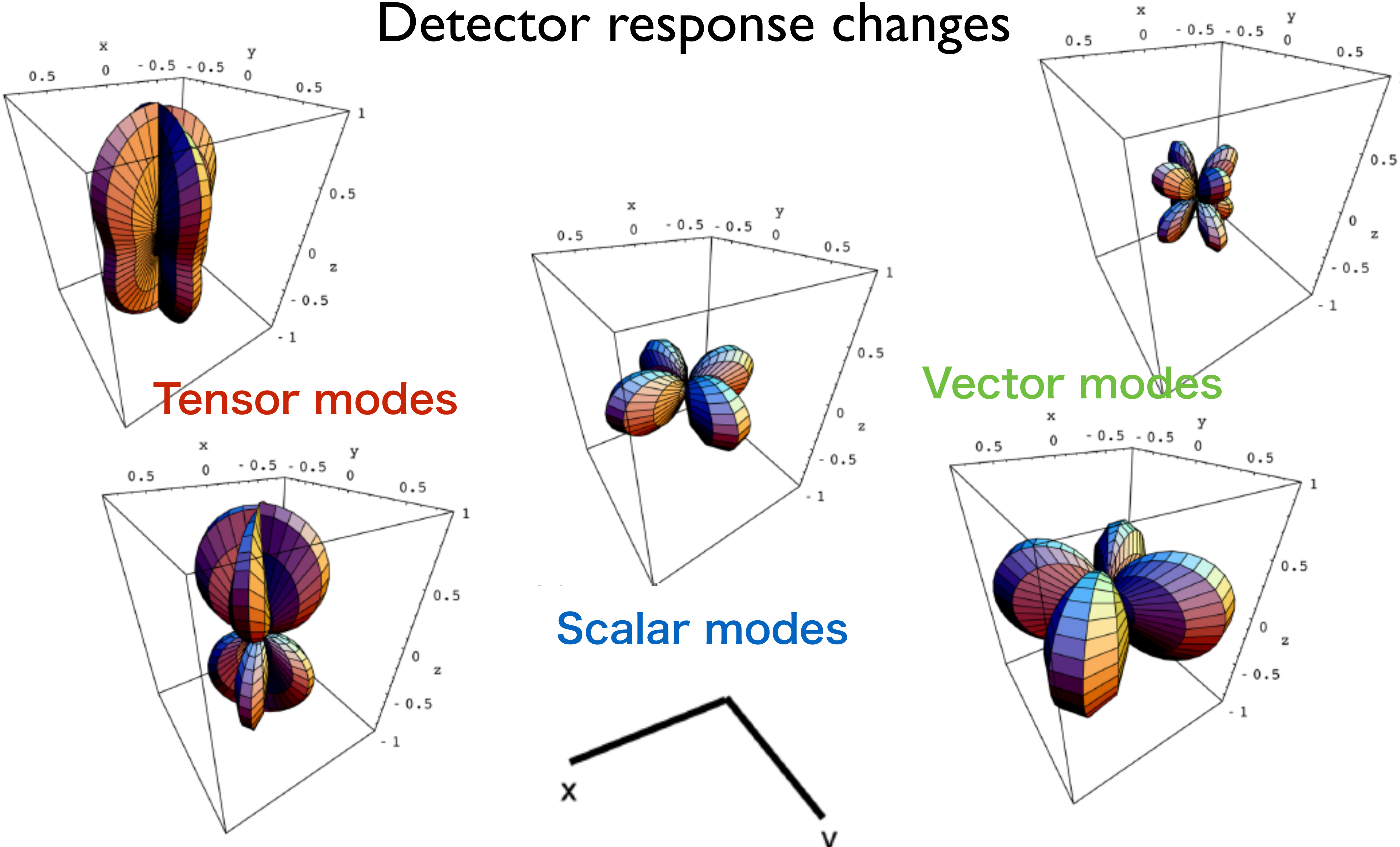

A. Nishizawa et al. PRD 79, 082002 (2009)

How can we detect polarization?

Overlap reduction functions

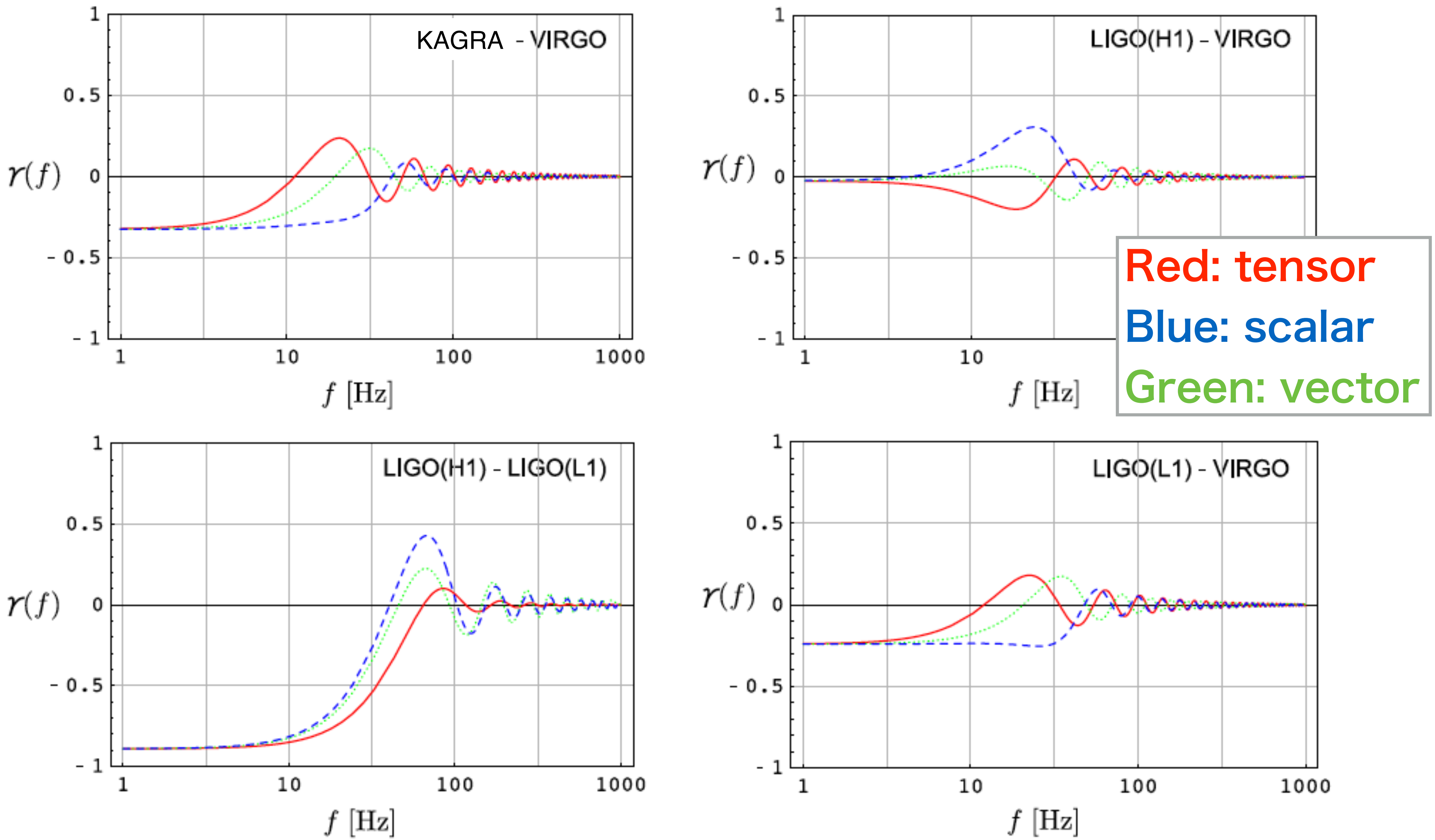

A. Nishizawa et al. PRD 79, 082002 (2009)

How can we detect polarization?

<u>Filter function</u>

overlap reduction function　　spectral shape template

$$\tilde{Q}(f) = \lambda \frac{\gamma(|f|)\,\Omega_{\rm gw}(|f|)}{|f|^3 P_1(|f|) P_2(|f|)}$$

noise spectra of detectors

→ We can extract additional polarization modes by changing γ(f)

A. Nishizawa et al. PRD 79, 082002 (2009)

KAGRA will help

O4 sensitivity curves (2021-)

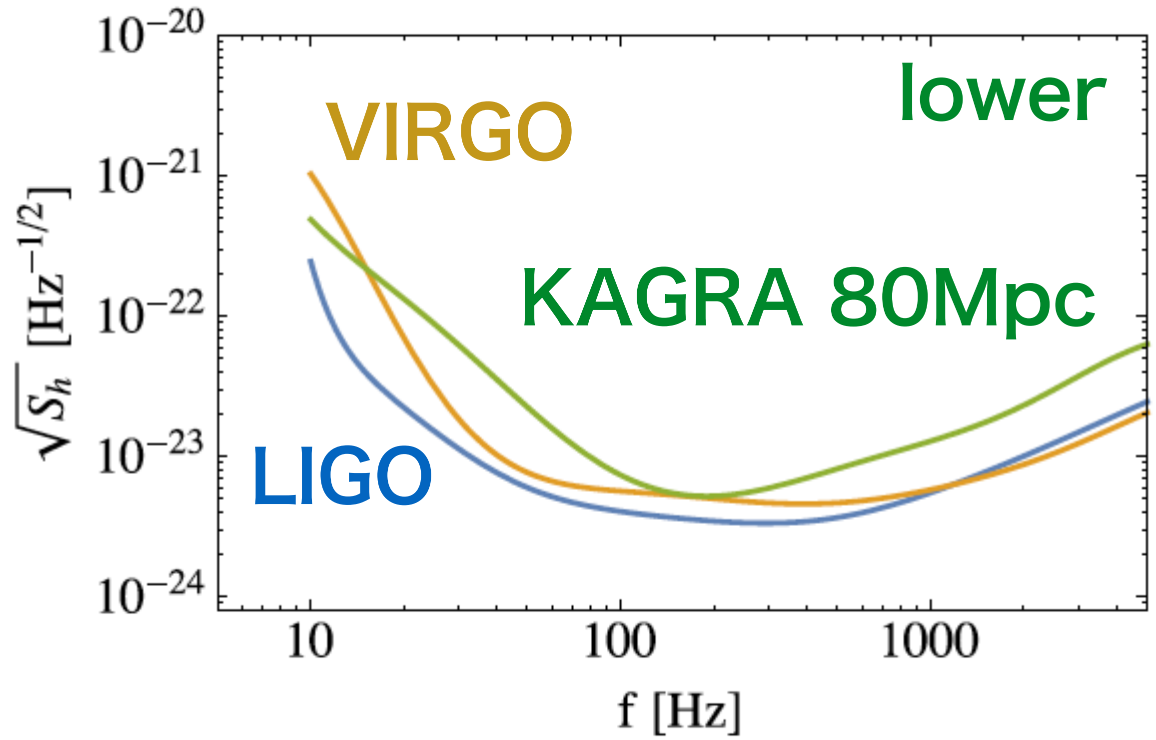

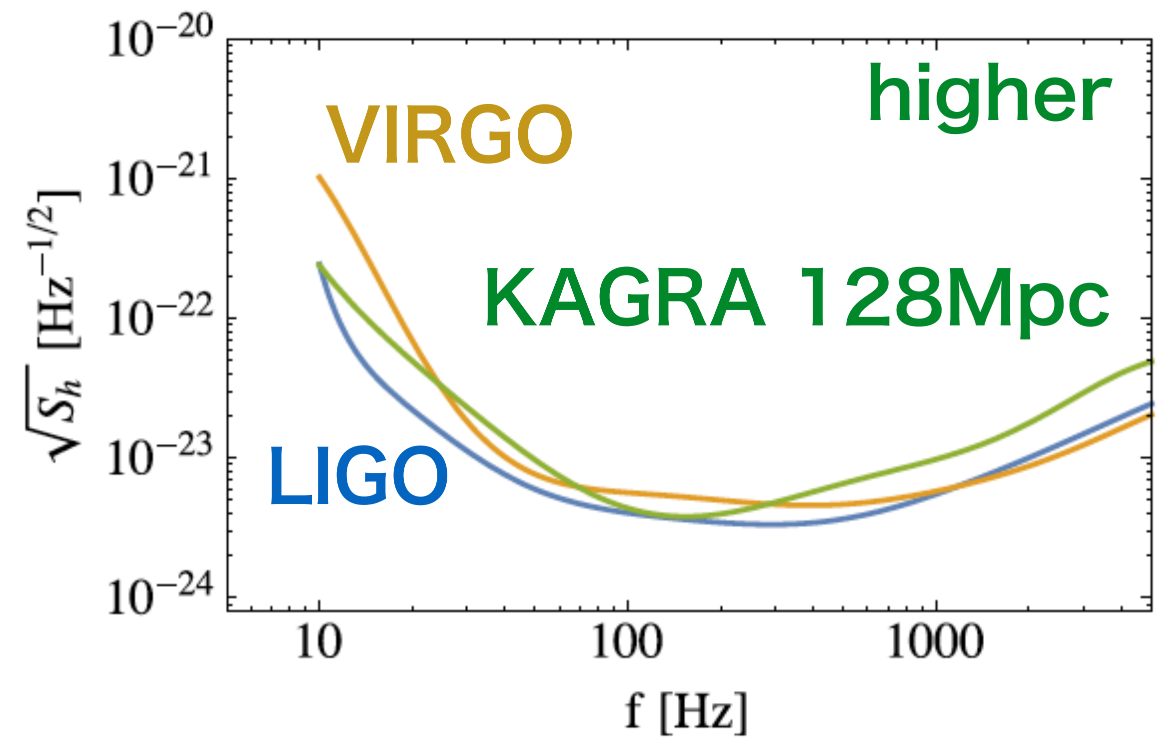

	$\Omega^T_{\rm GW}$	$\Omega^V_{\rm GW}$	$\xi\Omega^S_{\rm GW}$
LIGO×2 + VIRGO	6.6×10^{-9}	1.7×10^{-8}	8.3×10^{-9}
+ KAGRA (80pc)	1.3×10^{-8}	2.1×10^{-8}	1.4×10^{-8}
+ KAGRA (128pc)	5.8×10^{-9}	9.5×10^{-9}	6.6×10^{-9}

ongoing work with A. Nishizawa & G. Liu (KAGRA collaboration)

3. Anisotropy

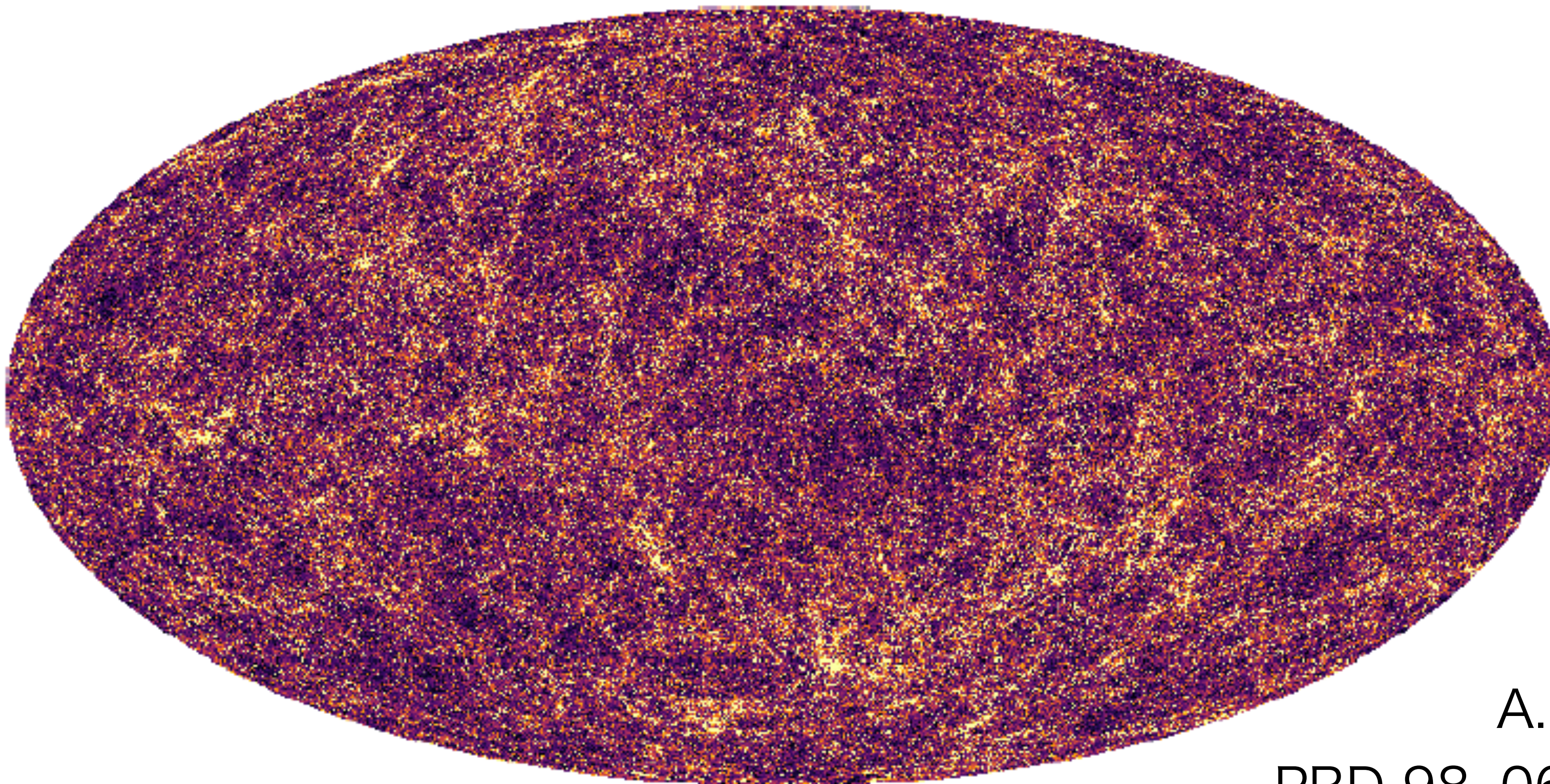

A. Jenkins et al.
PRD 98, 063501 (2018)

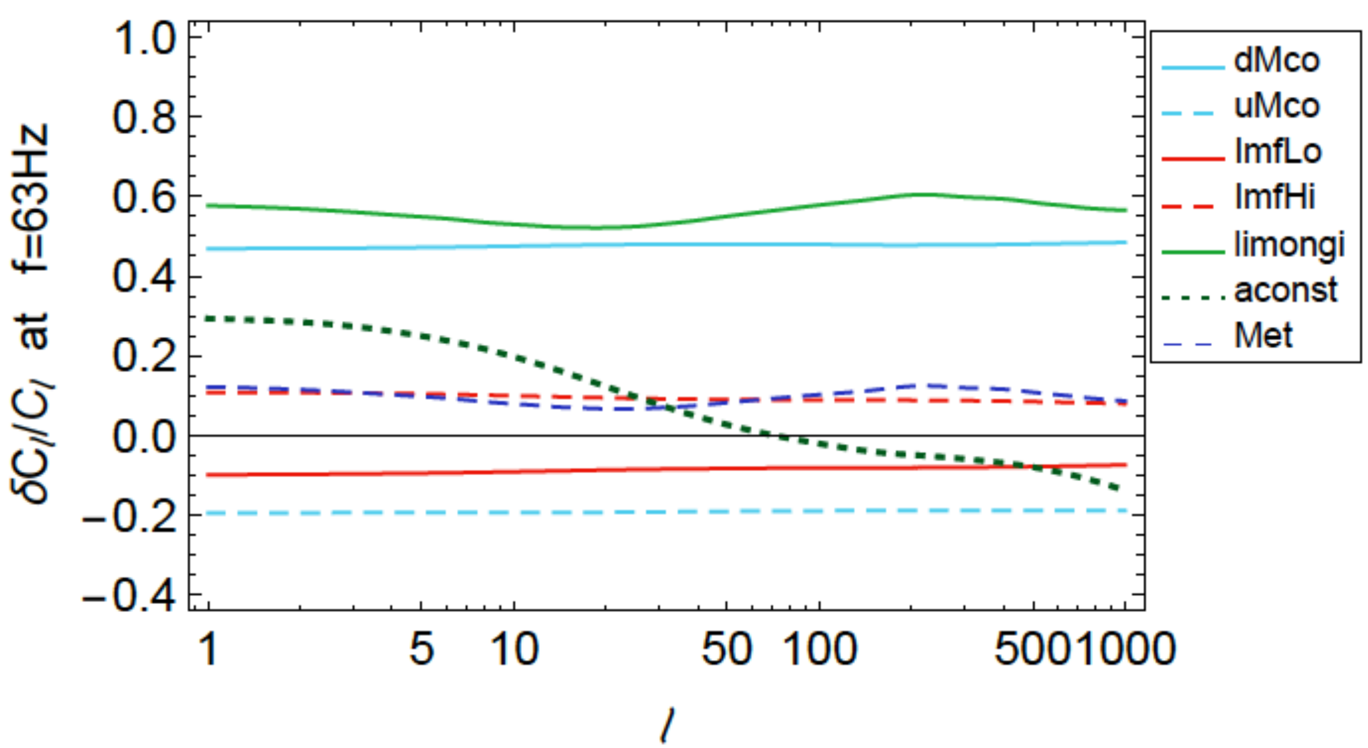

G. Cusin et al., arXiv:1904.07757 [astro-ph.CO]

Anisotropy of BBH GW background

→ helpful to distinguish between astrophysical and cosmological origin

How can we detect anisotropy?

Overlap reduction function changes

$$\gamma^T_{IJ}(f) \equiv \frac{5}{2}\int_{S^2}\frac{d\hat{\Omega}}{4\pi}e^{2\pi i f\hat{\Omega}\cdot\Delta\vec{X}/c}(F_I^+F_J^+ + F_I^\times F_J^\times)$$

isotropic GWs integrated over the whole sky

1. Radiometry

S. W. Ballmer, CQG 23, S179 (2006)

$$\gamma^{\hat{\Omega}}_{IJ} \equiv \frac{1}{2}e^{2\pi i f\hat{\Omega}\cdot\Delta\vec{X}/c}(F_I^+F_J^+ + F_I^\times F_J^\times)$$

→ filter for a point source in direction $\hat{\Omega}$

2. Spherical harmonics

B. Allen & A. C. Ottewell, PRD 56, 545 (1997)
E. Thrane, PRD 80, 122002 (2009)

$$\gamma_{IJ,lm} \equiv \frac{1}{2}\int d\hat{\Omega}\, Y_{lm}(\hat{\Omega})e^{2\pi i f\hat{\Omega}\cdot\Delta\vec{X}/c}(F_I^+F_J^+ + F_I^\times F_J^\times)$$

→ optimized for extended sources

4. Popcorn noise

Non-overlapping GW bursts

E. Thrane, PRD 87, 043009 (2013)

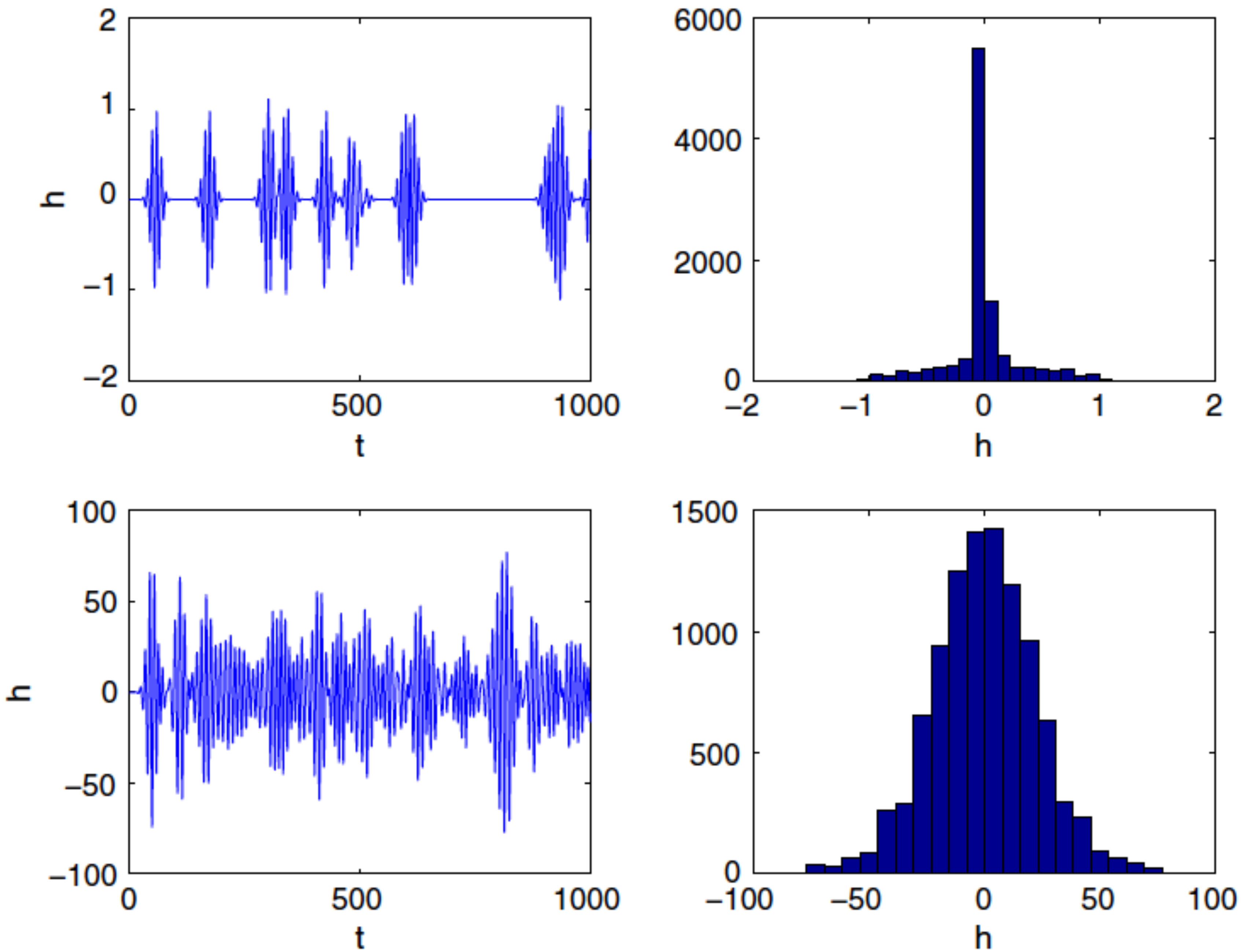

non-Gaussian distribution

Gaussian distribution

→ helpful to distinguish between astrophysical and cosmological origin

5. Non-Gaussianity

N. Bartolo et al. (LISA CosWG), JCAP 11, 034 (2018)

$$\left\langle h_{\lambda_1}\left(t, \vec{k}_1\right) h_{\lambda_2}\left(t, \vec{k}_2\right) h_{\lambda_3}\left(t, \vec{k}_3\right)\right\rangle = \delta^{(3)}\left(\vec{k}_1 + \vec{k}_2 + \vec{k}_3\right) \mathcal{B}_{\lambda_1,\lambda_2,\lambda_3}\left(\vec{k}_1, \vec{k}_2, \vec{k}_3\right)$$

- Overlapped astrophysical sources
- Sub-horizon-produced cosmological GWs

→ Gaussian (the central limit theorem)

- Inflation
- Topological defects (long strings)

→ could generate non-Gaussianity

But…

Propagation through large scale structure suppresses the non-Gaussian signal due to Shapiro time delay

N. Bartolo et al. PRL 122, 211301 (2019); PRD 99, 103521 (2019)

Summary

- There are various mechanisms to generate a **stochastic GW background in the early universe**.
- Once it is detected, it will bring a breakthrough in the understanding of our Universe
- Information beyond the amplitude of a GW background

1. **Spectral shape** → applicable to all origins
2. **Polarization** → probe of non-GR
3. **Anisotropy**
4. **Popcorn noise**

(3., 4.) → typically of astrophysical origin

(5. Non-Gaussianity) → inflationary models

→ Hints for discriminating origins